Universidade do Porto

Faculdade de Engenharia

FEUP

Computational tools for data fusion and signal processing of human gait

André Mendes Marques de Carvalho

MSc in Bioengineering

Porto, 2013

André Mendes Marques de Carvalho

Computational tools for data fusion and signal processing of human gait

Master thesis in Bioengineering

Supervisor: Prof. Dr. João Manuel R. S. Tavares

Co-supervisor: Doutora Andreia Sousa

Faculdade de Engenharia da Universidade do Porto

Porto, 2013

Acknowledgements

The work presented in this dissertation would not have been possible without the support and contribution of several people to whom I would like to address a special thanks:

- My supervisor, Professor João Tavares, for the availability, encouragement and support.

- To my co-supervisor, Andreia Sousa, for all the patience revealed during my visits, for all the opinions and shared resources.

- To my father for all the scientific support and help.

- To my family for being there whenever was needed and for encouraging me to follow my dreams.

- To all my friends who believed in me specially Rosa and Raquel.

Abstract

One of the most common motor actions is gait control. This is of critical importance and is highly affected by factors such as somatosensorial inputs, ground inclination and health problems. The goal of this study is to provide some computational tools for helping the analysis of electromyographic (EMG) and ground reaction force signals recorded during gait. The EMG signal will be analysed both in the time domain with classical techniques (wRMS / envelope) and also in the frequency domain, where patterns of muscle activation are expected to be found during cyclic movements. The ground force signals will be subjected to a classical analysis to provide the full centre-of-pressure (COP) and centre-of-mass (COM) kinematics as well as compute external power and work by both the independent and combined limb methods.

The main concern was to provide correctness in all equations and coding, secondly to provide new analysis tools and lastly to make the code as simple to use and modify as possible.

Some of the tools used (wavelet analysis) are computationally demanding so some optimization effort was done on the standard tools to provide one to two orders of magnitude improvement on these particular datasets.

Of course, having done the time-frequency analysis, the code also offers some trivial quality diagnostics on the EMG signal.

Finally, using the available dataset, some global analysis is presented.

Hopefully these tools will be of any help to the health professionals.

Index

List of figures

List of Tables

Abbreviations

COM – Center of mass

COP – Center of pressure

EMG – Electromyography

GRF – Ground reaction forces

RMS – Root mean square

wRMS – Windowed root mean square

1 – Introduction

1.1 – Overview

Gait analysis is frequently referred as having started with Aristotle's works on biology (Aristotle n.d.).

Borelli is also frequently quoted in this context (Borelli 1680-1681) although the decisive component for bio*mechanics* was published a little later (Newton 1687) and so was not present in Borelli's works.

Nowadays, Gait Analysis is a standard subject of almost every course in Biomedicine, Biomechanics, Physiotherapy, Sport, etc. PubMed quotes 11569 papers on the subject since 1977, with 1054 published in 2012. Google Scholar provides around 687000 hits on books, papers and thesis worldwide, with 14700 just in 2013.

In fundamental research, the final goal is, often, to understand the mechanisms associated with gait control. However, today gait analysis has evolved to a clinical tool where it is used to aid in surgical planning on cerebral palsy cases (DeLuca, Davis et al. 1997; Cook, Schneider et al. 2003; Lofterod, Terjesen et al. 2007), assess the efficacy of surgical interventions, evaluate the rate of deterioration in progressive disorders or evaluate the impact of medication and orthopedic aids (Pollo 2007). Quantitatively, it is used to identify gait patterns, speed of walking, mechanical work made by the main muscular groups during the diverse phases, etc. (Sousa 2009).

In order to study these mechanisms a range of data collecting devices can be used: force plates for registering the force exerted on the ground, EMG for detecting the muscular activity, video cameras for visual tracking particular anatomical points, accelerometers/gyroscopes and LIDAR for body part kinematics and many other techniques.

The array of raw data is usually combined to obtain the kinematics and dynamics of a particular joint, the time evolution of the contact with the ground (centre of pressure) or the time evolution of the centre of mass. EMG aims at providing directly the muscular activity and both time techniques (windowed standard deviation) and frequency techniques (spectral content, filtering, etc) are usually employed for processing. Also some integration of the multiple data streams is also necessary (data fusion), at least synchronizing and overlapping records.

These aspects are to be detailed in the next few pages.

1.2 – Objectives

To produce a set of computational tools to aid medical and para-medical staff in accessing patients with gait-related disorders. These tools are to be written in a language easily accessible to health professionals and must address the main data sources: multiple ground reaction force sensors and multiple surface EMG sensors. Data quality should be checked whenever possible. All output should be made available onscreen and also on a (cumulative) file for offline processing.

1.3 – Structure

The present work is divided into five chapters. In the first one a general overview of the work is made and its objectives are defined. In chapter two it is explained how an action is performed and the particular case of gait. The two major human gait theories are also described. In the third chapter a description of the material is made. It is explained how the EMG and force plates works and the physical meaning of their signals. In chapter four we explain how the code was developed, the choices made, it's assumptions and efforts made to reduce computation time. Finally the conclusions and future developments can be found in chapter five.

1.4 – Main contributions

There are three main (original) contributions for this thesis:

- The fusion of data from a double force plate setup allowed the computation of all kinematic quantities of both the COP and COM with high accuracy and without the need for any other sensors or data.
- The implementation of a wavelet based EMG signal processing strategy is original and unpublished (as far as we know) and may allow for the detection of activation phases regardless of any adaptive RMS voltage threshold.
- The optimization of a (specific) wavelet transform package allowed for reasonable processing times in commodity grade computers.

The first one – that can be extended to 3-step systems - allows quantitative studies on gait stability and other health related issues like prosthetic, chirurgic, drug or physiotherapeutic influence on gait recovery.

The second one explores the interest in avoiding EMG intensity-based inferences as they depend on location, muscular dynamics and quality of skin-sensor interface. As there are almost no non-linear effects, frequency-based techniques are insensitive to all of these, allowing for a generic activation detection strategy. The

proposed idea is implemented but needs validation studies has we had almost no time (and available data) to test it.

The third one is much less *bioengineering* but was a hurdle needed to be overcome to allow the implementation of the wavelet time-frequency decomposition idea. Even if proved good, extreme computation times would make that idea unusable to the common health professional or even researcher.

Several other minor contributions are scattered throughout the code. As no code has been reused from any source (except the profoundly optimized wavelet transform) and algorithmic choices and implementation details are not inspired on any paper, book or software, they are all original contributions, but are mostly trivial consequences of the current state of the art and so are not included here.

Chapter II – Basis of human movement

2 – Basis of human movement

2.1 – Introduction

The complexity of the motor system is reflected on the complexity of the actions humans can achieve (Enoka 2008). These actions are a result of the interactions between the musculoskeletal and nervous systems, the first acting as a support and the second as the coordinator (Ghez and Krakauer 2000). Being so, all movement is achieved by the coordinated response of the muscles to neural commands (Bawa 2002).

Some of the most common motor action are the postural control and gait control. The postural control is a rather complex skill based on the interactions of dynamic sensory-motor processes and can be separated into two main functional goals: the postural orientation and postural equilibrium (Horak 2006). As for the Gait control this is a complex action in which the body COM is continuously unbalanced so the body weight is transferred from one leg to another with the minimum energy consumption (Alonso, Okaji et al. 2003).

For a motor action to take place it is needed a proper alignment of all body sections so it can maintain its stability despite all the unbalancing forces (Mackey and Robinovitch 2006). This way motor control can be defined as all the processes from which the nervous system, based on visual, vestibular and somato-sensory inputs, controls the musculoskeletal system to create coordinated movements and skilled actions while maintaining body posture (Júnior and Barela 2006).

The main goal of this chapter is to make a small explanation on how gait works, the main gait theories and what is a typical gait pattern.

2.2 – Gait

The primary goal of walking is the locomotion of the body from one place to another. To achieve this humans alternate their support from one leg to another, always keeping one foot on the ground, in an action where the body center of mass is displaced from its regular position allowing for the body to move forwards. The movements that take place during walking are cyclic and optimized to decrease energy expenditure (Silva 2009).

During regular walking a person needs to be able to maintain movement patterns, be able to maintain a dynamic equilibrium between the body center of mass and the moving support and to change his movement pattern in response to any external disturbance. The Walking cycle is every movement that occurs between the

initial contact of one foot in the ground and the instant that foot touches the ground again (Monteiro 2004).

Each walking cycle has two steps, one for each leg, and it is divided by two main actions, the support and the swing (Figure 1). The step refers to the contact between the foot and the ground and it correspond to 60% of the cycle time. The swing corresponds to the other 40% and is the time in which a leg is progressing thru space (Rose and Gamble 1998).

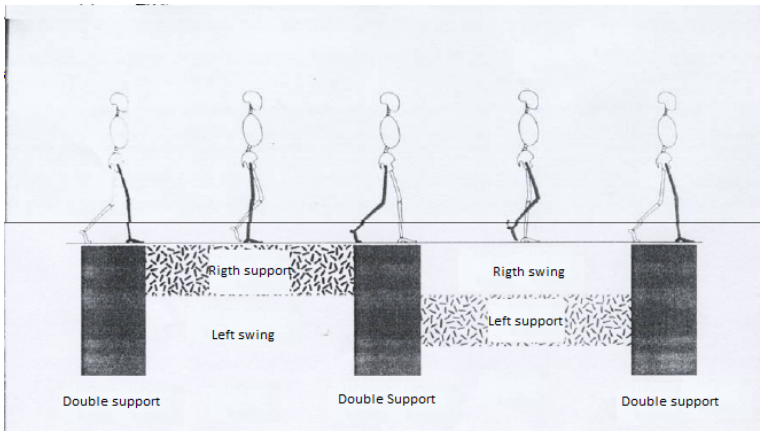

Figure 1 - Walking cycle [adapted from (Perry 1992)]

As to the mechanical forces during gait there are two types: internal and external. The external forces are the gravity and ground reaction force (which can be measured with a force plate). Acting to oppose those forces are the internal forces. The internal forces corresponds to all the forces exerted or absorbed by muscles, ligaments, tendons and bones that work in order to counterbalance the external forces and support the body weight (Norkin and Levangie 1992).

During gait the COM describes a sinusoidal trajectory in the lateral and vertical displacements with 2 maxima in the vertical plane (two wave cycles) corresponding to the COM above COP for every step and one full wave cycle for the lateral displacement corresponding to the transition of the COP from one leg to another (Gard, Miff et al. 2004)

2.3 – Gait theories

The two prevailing models on human walking are the *inverted pendulum* and the *six determinants of gait* (Saunders, Inman et al. 1953), shown schematically in Figure 2. The six determinants of gait are the (proposed) set of 6 sub-actions of each step that seem to minimize the energetic cost of locomotion by reducing the vertical

and lateral displacement of the COM. They are the *pelvic rotation*, *pelvic tilt*, *knee flexion in stance phase, ankle flexion/extension mechanisms, knee mechanisms and lateral displacement of the pelvis*. The last one reduces the lateral displacement of the COM while the others reduce the vertical displacement. Unfortunately a closer look at the gait process showed that some of the *determinants* did not reduce the waving movements of the COM and also that a voluntary reduction of these movements increased the energy expenditure (Kuo and Donelan 2010). The coexisting inverted pendulum theory states that it is energetically benefic for the supporting leg to remain rigid creating an inverted pendulum, where the kinetic energy is converted into potential energy and vice versa. Unfortunately this model does not predict any energy expenditure at all during walking and is geometrically inconsistent during the double support phase.

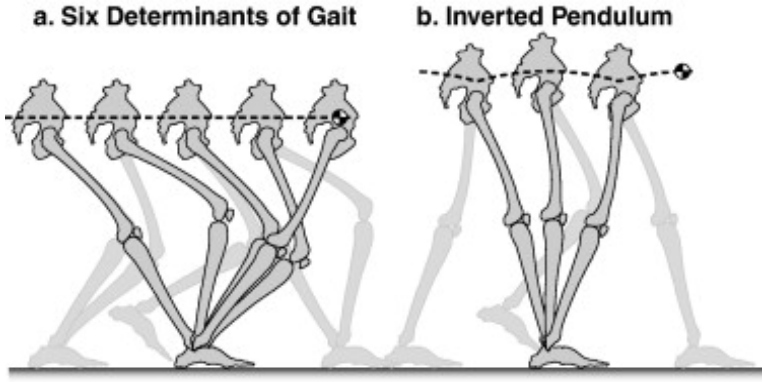

Figure 2 - Two major walking theories (Kuo 2007)

A little more realistic and less known theory is the *passive dynamic walking theory* (McGeer 1990), that sophisticates the inverted pendulum theory by incorporating the details of the heel-strike collision with ground. The author provided simulations and robotic samples proving the system is capable of passive stable locomotion on a small slope (downwards) and later others demonstrated that robots based on this model can move in flat ground with minimal energy expenditure (Collins, Ruina et al. 2005).

A model agnostic (phenomenological) approach divides the step into four phases: (i) ground strike, in which the foot touches the ground with much positive work from the quadriceps; (ii) the pre-load, in which the elastic energy is stored into the Achilles tendon and the quadriceps continue doing positive work; (iii) the propulsion, with major positive work done by the anterior tibialis; (iv) the swing, where no force is being exerted to the ground. In the swing phase, despite the absence of ground contact some muscular activity can still be found in anterior tibialis, hallucius and digitorum longus extensor (Norkin and Levangie 1992).

2.4 – Typical GRF gait patterns

The gait patterns can be influenced by almost any variable such as age, weight, diseases, strength, walking surface, etc. (Whittle 2007). Usually the gait patterns are obtained from force platforms that measure the ground reaction forces (GRF), equal and opposite to the ones made by the foot on the ground. Figure 3 is a representation of a typical healthy subject GRF pattern during half a walking cycle (between the pink bars). We can easily divide it in a (antero-posterior) breaking phase and an accelerating phase. For each leg, the point where no antero-posterior force is done (the location of the pink bars) is the point where the foot is under the hip (COP under the COM).

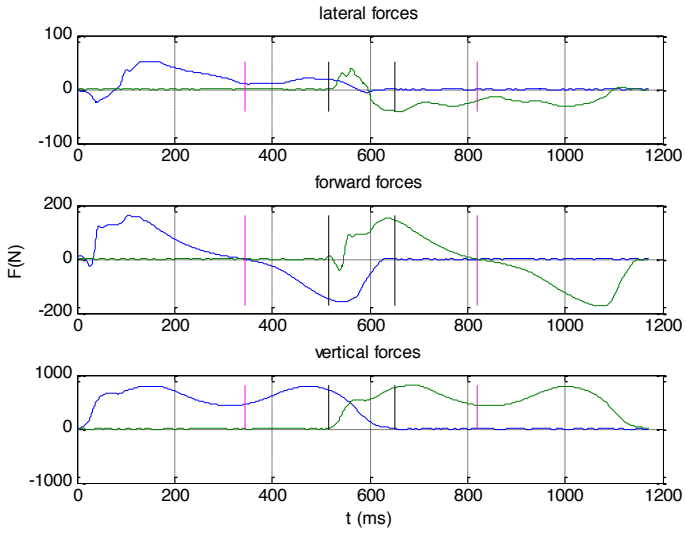

Figure 3 - Typical GRF gait pattern

The vertical component of the GRF reaches up to around 120% of the subject body weight. It has two maxima more or less corresponding to the two extrema of the antero-posterior curve. The first half corresponds to the force exerted to stop the descending movement of the COM and the second one corresponds to the force exerted to push the COM up again (Perry 1992).

The lateral component is usually the least studied of the three but can be used to investigate foot instability (Winter 1990).

When the full set of forces is known, we can time integrate them and compute the impulse (velocity variation times mass) and with another integration compute the COM displacement with remarkable accuracy. On the premise that the human body is not statically stable and that a control system is necessary to stabilize the body, it is frequent to study the time evolution of the COP and COM. We'll detail these a little later.

2.5 – Summary

Gait is a complex action that involves the precise coordination between the musculoskeletal and nervous systems, the first acting as a support and the second as the coordinator. This is a cyclic action optimized to minimize energy expenditure where the COM describes a sinusoidal trajectory in the lateral and vertical axis and whose support keeps alternating from one leg to the other.

There are two main gait theories, the inverted pendulum and the six determinants of gait. The first one are a set of 6 sub-actions of each step that seem to minimize the energetic cost of locomotion by reducing the vertical and lateral displacement of the COM and the second states that it is energetically benefic for the supporting leg to remain rigid creating an inverted pendulum, where the kinetic energy is converted into potential energy and vice versa.

The gait patterns can be influenced by almost any variable. These have very distinctive features and can be used to numerous studies. They can be obtained from force platforms that measure an equal and opposite force to the one made by the foot on the ground.

Chapter III – Instrumentation

3 – Instrumentation

3.1 – Introduction

Biomechanical instrumentations give us the ability to study gait and postural patterns as well as all the variables and diseases that can change a normal pattern increasing energy expenditure and increasing the probability of a fall. This is especially important for elderly people as this is one of the major causes of death and health related problems (Stevens, Corso et al. 2006). It also allows to quantify motor impairments and to keep tracking of diseases progressions. This kind of instrumentation is also used in rehabilitation to monitor improvements on stroke patients.

To study the gait and postural control mechanisms, a large array of instrumentation is available, including force plates, feet pressure sensors, EMG sensors, inertial sensors, video processing systems, EEG, radar, LIDAR, eye tracking systems and many other techniques. However the force plate is almost universal as it gives us simultaneously the COP location and (with some math) the COM time evolution, allowing for a quantifiable measure of body stability and control.

It is known that ageing, injuries, footwear and many others factors contribute to an abnormal postural and gait pattern. As the feet reaches the ground in different angles or as the center of mass displaces from its regular position the stability movements required to hold the body change. Consequently, force plates must be dissimulated not to induce changes in normal gait.

To have some idea of the mechanisms used for body control, it also frequent to use surface EMG sensors. These are non-intrusive and will give a (very) rough idea of individual muscular action, allowing for a more detailed study of the *control* aspects of locomotion.

In this chapter we will discuss the main equipment used to analyze gait such as EMG and force plates, as well as the physiological principles behind an EMG signal. A brief explanation on how the EMG signal processing is done using wavelets is also made.

3.2 – Force plate

There are several types of force plates depending on its transducers. The most popular are based on Hall effect probes, strain gauges and piezoelectric crystals. They are all thermally sensitive sensors.

The Hall effect sensor produces a voltage as a response to a magnetic field, usually from a nearby magnet. They must be driven by a stable current and a voltage must be measured with high impedance. They are rugged devices but are not very accurate, can’t be used near power cables, etc..

Strain gauges change electrical resistance according to mechanical elongation. They are measured usually with a bridge setup but the current changes the electrical resistance so a warm-up time is needed. They are fairly accurate but don't age well (the bonding of the sensor to the supporting metal moves) and so need regular recalibration.

Piezoelectric is a charge sensor, sensitive to elongation. Piezoelectrics have a wide sensing range and frequency response as well a very good linearity and aging properties and so are used from ultra sensitive devices (microphones) to high load devices (sensors between the car and the wall in car crash tests). However they are expensive, sensitive to external vibration and demand electrometer amplifiers.

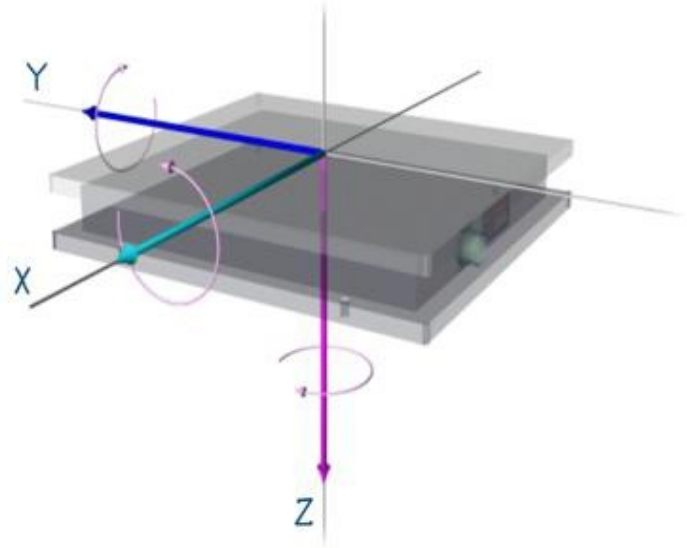

Figure 4 - Force platform and measured force components (Pais 2005)

The most common force plates have six sensors to measure the three force components and the three torque components as shown in Figure 4 (each sensor is one-dimensional, so at least 6 are needed).

Figure 5 - Force plate components (AMTI 2013)

Force plates usually have a non-serviceable embedded pre-amplifier system and also an external amplifier box, where the user can set the gain applied to each physical sensor (Figure 5) and switch on and off some filters (notch at line frequency,

low pass for anti-aliasing and force plate resonant frequency avoidance, etc). Of course the gain must be small enough as to not saturate the signal but as high as possible to minimize the quantization noise. The analog signal is then feed to an ADC and routed to a computer where a software tool manages the data acquisition and storage.

In order to transform the sensor information in force and torque measurements a simple linear transformation is performed, including the information of the amplifier gains. An example of a correct final signal recording can be seen on Figure 6.

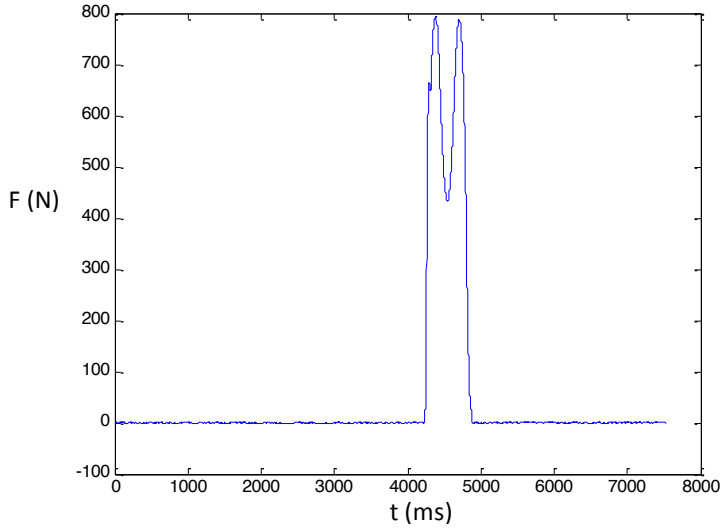

Figure 6 - Force plate signal (vertical GRF)

Common problems can be seen in Figure 7 and Figure 8 and both preclude the usage of this data any further.

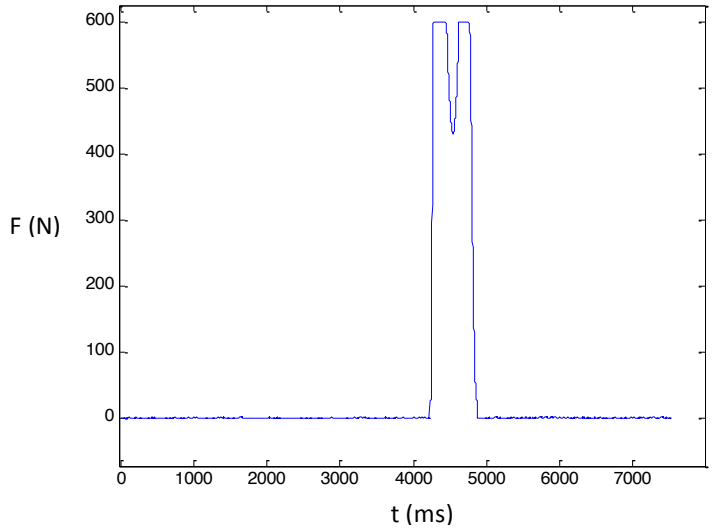

Figure 7 - Channel saturation (excessive gain)

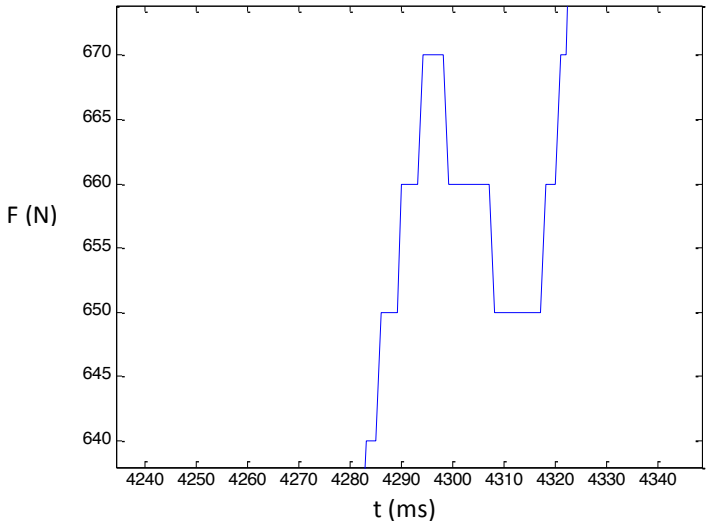

Figure 8 - Quantization noise (small gain)

3.3 – Electromyography

EMG history can be traced back to Redi's experiments (Redi and Platt 1686) on electric eel muscles. He found that electric eels have a highly specialized type of muscles that can produce electricity. One hundred years later (Fowler and Galvani 1793) a series of experiments were conducted that demonstrated that muscular contractions could be induced by the discharge of static electricity. Later (Du Bois-Reymond 1848) the first evidence of electrical activity during voluntary contractions in human muscles were recorded using a galvanometer. In 1950 appeared the first commercially available electromyography system and subsequently the EMG field faced significant developments with the contributions of numerous researchers and the growing capabilities of the semiconductor industry (Ladegaard 2002)

The activation/deactivation of each muscle fiber generates an electrical field that can be measured - the electromyographic signal (Basmajian and De Luca 1985). This way a direct measurement of the muscular activity can be made: the degree of muscular activation, the rate of force production, the number of motor units recruited, etc. However it is impossible to sense all muscle fibers in a muscle, much less in the body. So a few main muscles are selected and a single *surface* EMG probe is used in each one. Theoretically the *surface* EMG signal would correspond to the sum of all motor units action potentials (supra citæ). But each fiber signal crosses different tissues and impedances (changing in time) and other sources contaminate this as well, also dynamically. In order to better understand the quantities measured by the EMG first we need to understand how the muscle works.

3.3.1 – Muscular system anatomy

The human body has over 600 skeletal (voluntary) muscles. Each one is a hierarchical structure that contains fascicles, muscle fibers, myofibrils and *actin and myosin* filaments as shown in Figure 9.

Each of these structures is surrounded by connective tissue as well as blood vessels and neurons (sensing). The connective tissue that holds the muscle together is called the epimysium, the one that covers the muscular fascicle is called the perymisium and muscular fibers are involved in the endomysium. Muscle fibers can be further decomposed into myofibrils, sarcoplasmatic reticulum and T-tubes as seen on Figure 10. These are of fundamental importance during muscular recruitment.

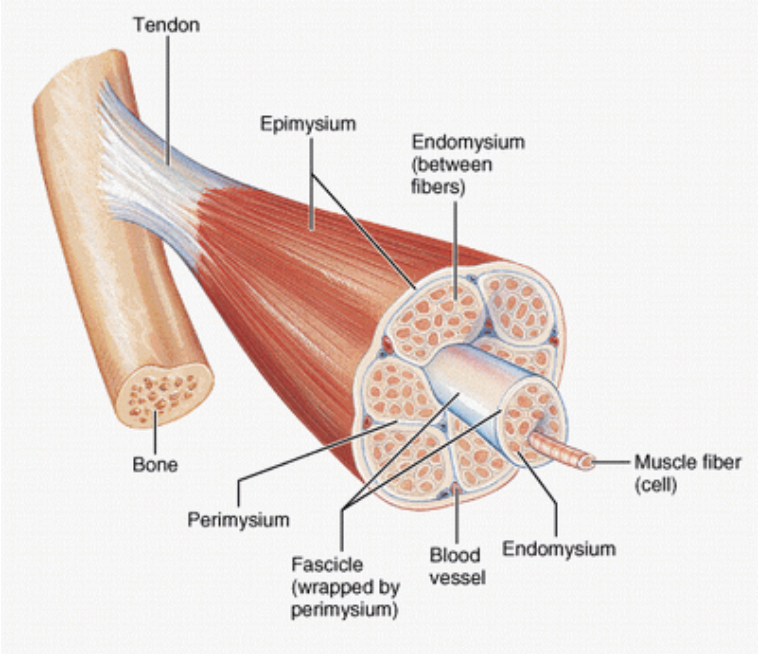

Figure 9 - Schematic of muscle components (MedicaLook 2013)

Each of these structures is surrounded by connective tissue as well as blood vessels and neurons (sensing). The connective tissue that holds the muscle together is called the epimysium, the one that covers the muscular fascicle is called the perymisium and muscular fibers are involved in the endomysium. Muscle fibers can be further decomposed into myofibrils, sarcoplasmatic reticulum and T-tubes as seen on Figure 10. These are of fundamental importance during muscular recruitment.

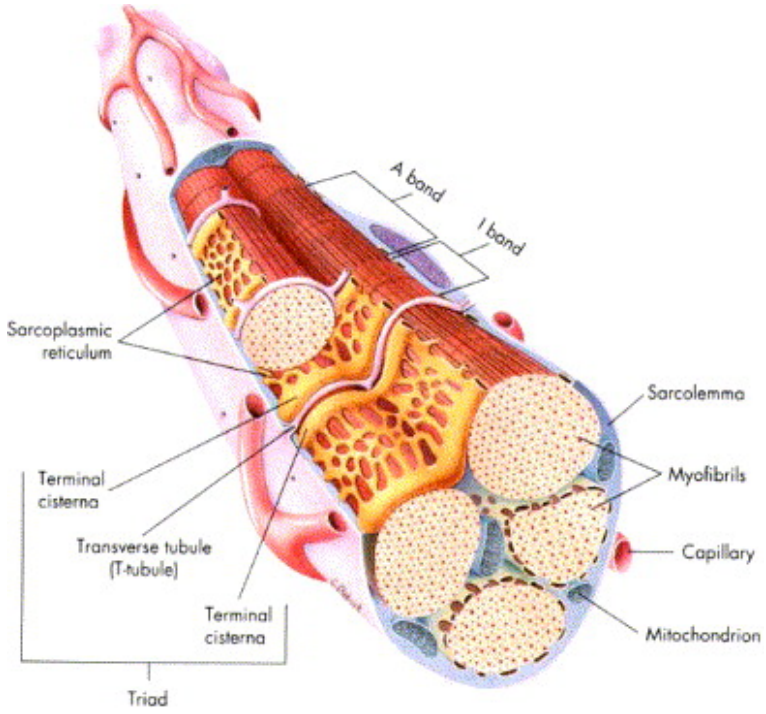

Figure 10 - Muscle fiber structure (Seeley, Stephens et al. 1995)

The myofibrils are formed by highly organized sub-units called the sarcomers that are placed continuously on top of each other. This is the unit that's responsible for the contraction of the muscle. The sarcomere is made of various regions and 2 major types of bundles, actin and myosine filaments that alternate with each other (Figure 11).

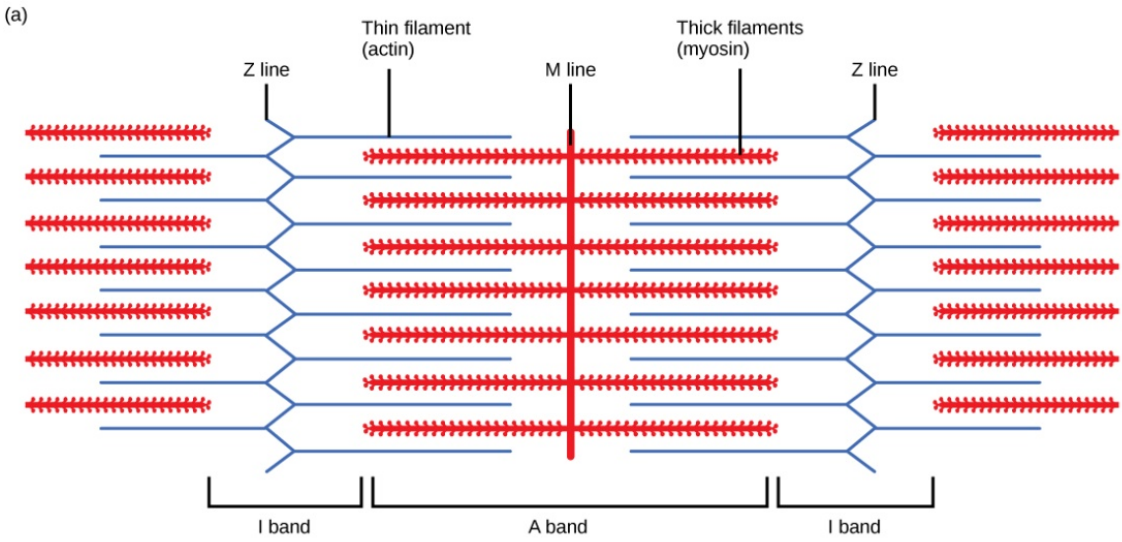

Figure 11 - Sarcomere representation (ProProfs 2013)

As shown in Figure 12 the actin filament is made of actin monomers, that have a specific binding site to the myosin molecules, and are fold in a double helix structure. They are also made of chains of an elongated molecule called tropomyosin that are placed above the actin binding sites and can cover up to seven actin molecules at once. The troponin is the last molecule of this complex and has 3 sub-units, one that binds to actin, other to tropomyosin and other to calcium ions.

The myosin filaments are made of numerous myosin molecules that have a golf club shape-like appearance. These molecules are made by two heavy-chain and four light-chains myosins.

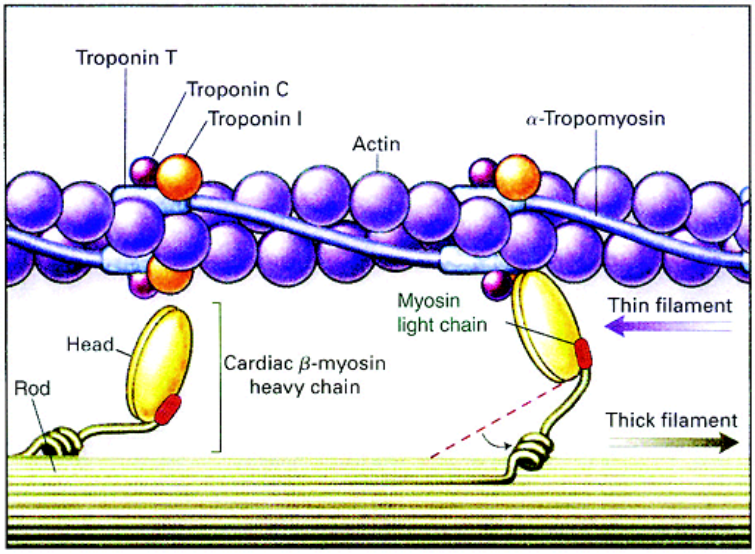

Figure 12 - Actin and myosin schematics (Kamisago, Sharma et al. 2000)

3.3.2 – Motoneuron

For a contraction to take place several structures of the nervous system must be involved. At the end of the central nervous system, in the spinal cord, specialized neurons (moto-neurons) connect with sets of muscle fibers and initiate the contraction (Kernell 2003). These sets of muscle fibers (Figure 13) are the minimum unit that can be recruited at any given moment and are called the motor unit.

Once a motor neuron is activated it generates a potential difference in its innervated muscle fibers resulting in an action potential (Figure 14). This happens every time an unbalanced distribution of ions inside and outside the cells is achieved (Loeb and Ghez 2000).

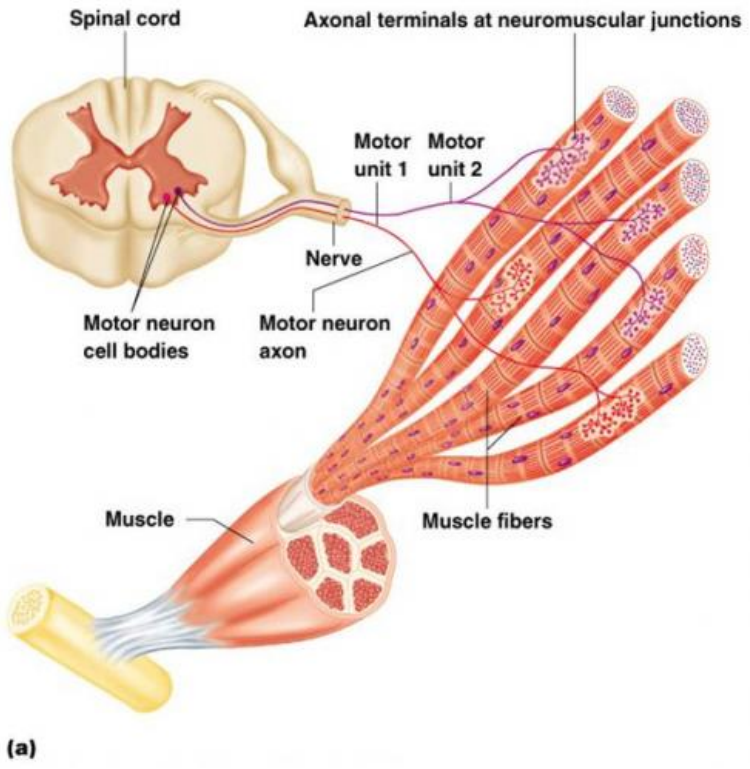

Figure 13 - Motor unit schematics (BaileyBio 2008)

3.3.3 – Action potential

At rest, cell membranes are polarized (-70 to -90 mV) due to an excessive concentration of negative ions inside and positive ions outside the cell. This is a result of the good permeability of the membrane to the potassium ions and poor permeability to the negative charged ions.

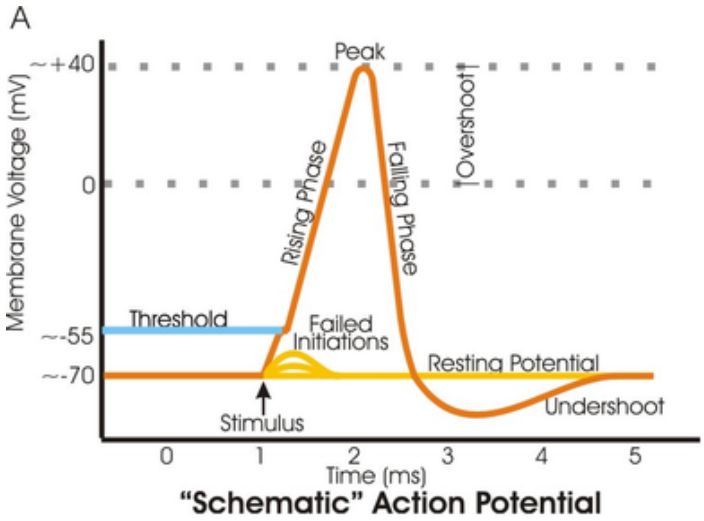

Figure 14 - Membrane potential of a muscle cell (Wikipedia 2005)

Once a cell gets sufficiently stimulated by the axon of the motor-neuron, an action potential occurs. This stimulus opens the sodium channels and the influx of sodium thru the membrane (osmotic pressure) will equalize potentials and even raise it up to +40 mV. This ion migration and potential change is a local effect that will affect the next sodium channels in the membrane, and then the next until the end of the fiber is reached. This is a propagating depolarization wave, from the enervation point to both ends of the fiber. Shortly after the opening of the channels they will close again and the potassium channels will finish expelling potassium from inside the cell, returning the membrane to its rest state(Seeley, Stephens et al. 1995).

3.3.4 – Neuromuscular junction

The neuromuscular junction is the region where the axon of the motoneuron connects to the muscle fiber creating a synapse (neuromuscular junction). The gap between the muscle fiber cell membrane (sarcolemma) and the axon terminal is called the synaptic cleft, Figure 15. Once an action potential reaches the axon terminal the calcium channels opens and calcium enters inside the axon cell membrane. This leads to the secretion of the content of several presynaptic vesicles within the synaptic cleft. The acetilcoline molecules bind to specific receptors on the within the postsynaptic membrane that allow sodium to get thru leading to an action potential in the muscle fiber.

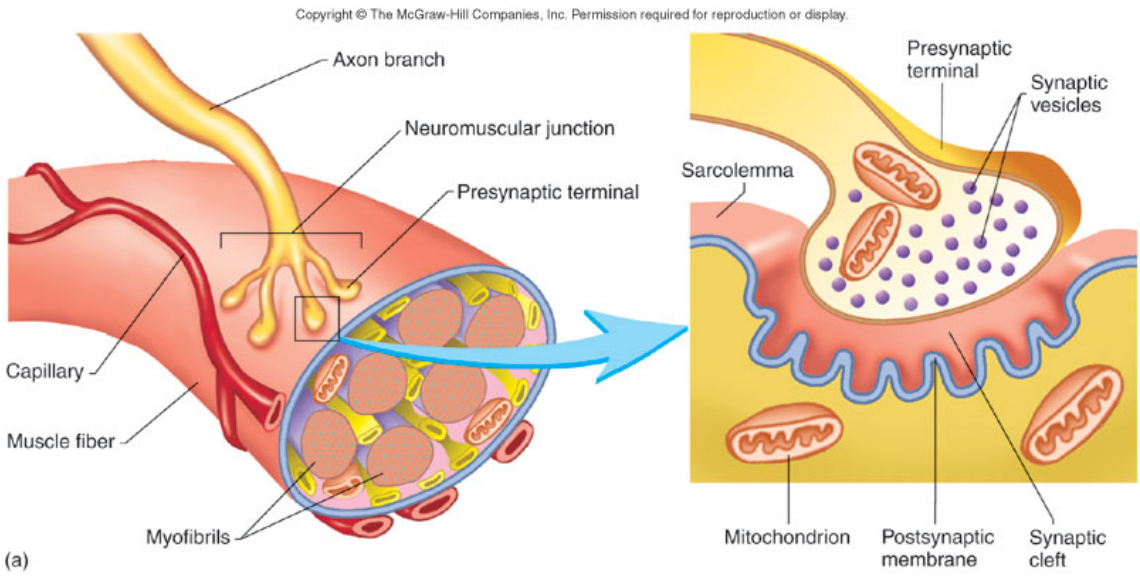

Figure 15 - Synapse (Seeley, Stephens et al. 1995)

3.3.5 – Muscle contraction physiology

Once the action potential reaches the synapse another one travels throughout the entire muscle fiber. Every time this reaches a T-tubule the calcium channels on the sarcoplasmic reticulum opens and the calcium stored in the sarcoplasmic reticulum enters the sarcoplasm. The calcium ions bind to the troponin that causes the tropomyosin to rotate exposing the actin binding sites. This leads to the binding of actin and myosin head that pull the actin filaments (Figure 12). This action is repeated during the contraction in every sarcomere within the muscle fiber until the H zone disappears, Figure 16.

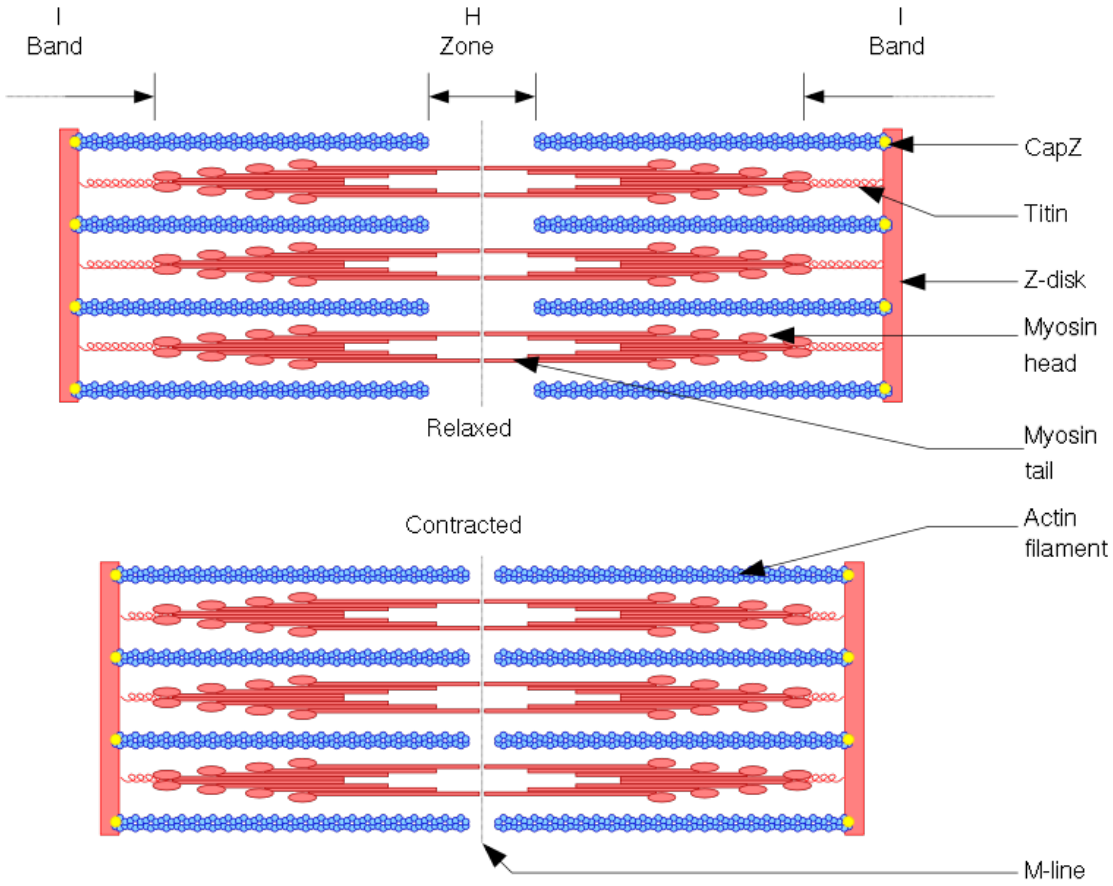

Figure 16 - Sarcomere changes during muscle contraction (Wikipedia 2007)

3.3.6 – Force production

If a motoneuron stimulus is strong enough to cause an action potential in its innervated fibers then all of them will contract as much as they can. This is called the all-or-none principle. During muscular contraction an increase in the force exerted by the muscle can be achieved in two ways. More muscle fibers can be recruited at any given time and/or each fiber (motor unit in fact) can be fired more often per unit of time. The first way of increasing force production is by increasing the strength of the

stimulus. This will increase the number of motor units recruited which in turn will increase the number of muscle fibers activated. The second way is related to the way the muscle fiber contracts. If a muscle fiber is stimulated a contraction occurs and shortly after it starts to relax. This means that the time averaged force exerted by that muscle fiber will be small. With the increase in the recruitment frequency so does increase the average force produced. Tetanus is the frequency above which the average force is maximum i.e. a new stimulus is sent even before the fiber is completely depolarized.

3.3.7 – EMG electrodes

The electric signals associated with muscular activity can be detected using EMG. There are two major types of electrodes, intramuscular and surface electrodes (Farina, Merletti et al. 2004) as shown in Figure 17. The intramuscular electrodes are used to study individual motor units. They are introduced with a needle and they get in direct contact with the muscles fibers. The main problems regarding intramuscular electrodes are the limited amount of muscle fibers that it can detect and the inconvenience related to invasive methods (Basmajian and De Luca 1985).

Figure 17 - EMG electrode examples [(Medizintechnik 2013) and (Bio-Medical Instruments 2013)

As for the surface electrodes they are painless and have a larger area of detection. They deliver the sum of all the electric activity on the detection area, allowing the study of the global activity of a muscle. Its main disadvantages are its inability to recover the individual motor unit activity and its susceptibility to crosstalk, meaning that a vicinity muscle activity can be felt and promote misleading readings (Rau, Disselhorst-Klug et al. 1997). Almost universally EMG sensors are of differential configuration, strongly reducing the interference of power line induced noise.

3.3.8 – Surface EMG signals

As the EMG signal is of the order of tens of mV at the fiber, and one or two orders of magnitude less at the surface, amplification levels of 1000 to 10000 are common. To avoid interference, differential (or even multiple differential) systems are used, placing a pair of sensing elements along the fiber direction (pennation angle) one or two centimeters apart. Considering just one fiber, when the depolarization wave passes, it is seen twice with one of the lobes inverted Figure 18.

At the surface of the limb the signals from several motor units being recruited at different rates will arrive with varying delays and attenuations, producing the interference pattern that is recorded Figure 19

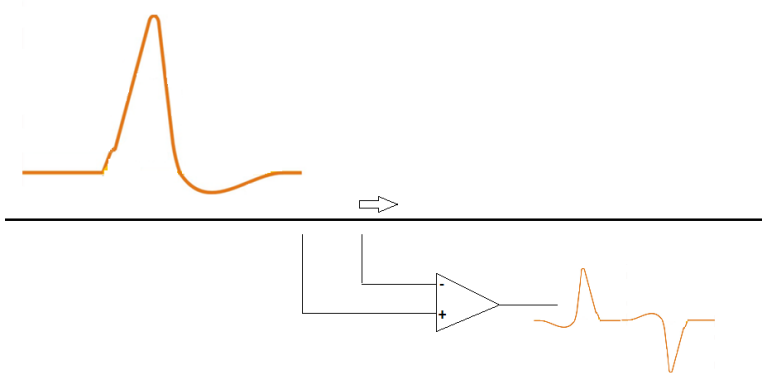

Figure 18 - Differential amplification of EMG signal

The recruitment or *firing* rate for any given fiber (motor unit) is just of a few Hz but each wave is spectrally richer than that, say up to a few hundred Hz. The usage of high-pass filters to avoid motion artifacts eliminates the possibility of recovery of the firing rates and so of an important part of the relation of EMG and force.

The different distances from each fiber to the sensor introduce different delays to each wave so that simultaneous depolarization waves (maximum force) will not produce a maximum amplitude signal. But some particular combination of firing delays (sub maximal force) can produce a simultaneous arrival of the multiple waves and produce a maximum signal. Additionally, if there is movement the muscle fibers will move relatively to the skin and the surface sensors, increasing the complexity of the conduction, summing and EMG interpretation process. And all the other muscles in the neighborhood will also produce signals that can interfere with the ones we are trying to record. So, at best, the EMG signal recorded with single differential methods at the surface of the skin has only a qualitative relation with the force produced by some muscle. Also no two muscles or two experiences can be compared as the location and the adhesion of the sensors to the skin is not identical.

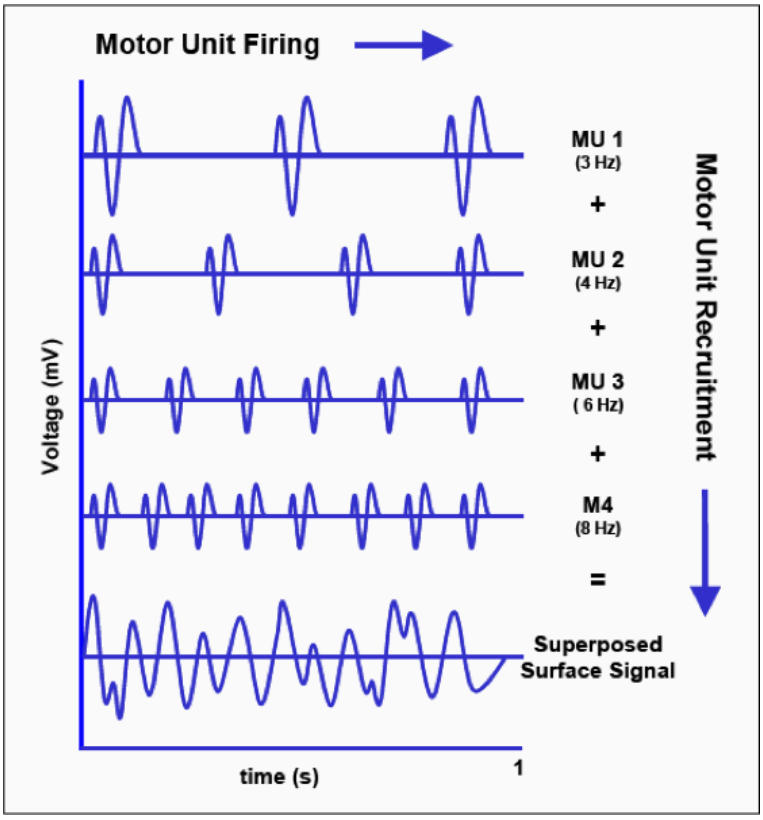

Figure 19 - Interference pattern (Quach 2007)

Usually the frequency of an EMG signal can go from 0 to almost 1kHz but with most of the energy being below 150Hz. As for the amplitude it usually has values ranging from 0.1 to 1 mV for surface electrodes (Basmajian and De Luca 1985). Due to the small amplitude and the sensitivity of the electrodes, the signal must be filtered, to avoid low frequency noise contamination, amplified and converted before it can be read by a computer or other processing unit. The EMG main noise sources are line noise (50Hz), motion artifacts (less than 20Hz) and inherent noise of the electronic components (Raez, Hussain et al. 2006). Typically embedded in the electronic system is a high-pass filter, used to cut the frequencies below 20Hz, and a low-pass anti-aliasing filter at the kHz range. A notch filter can also be used to reduce the power line noise contamination, but it will attenuate not only the desired frequency but the adjacent frequencies as well. Since dominant signal frequencies are also located in the 50-100Hz range the use of notch filters is not advisable at all (De Luca 2002).

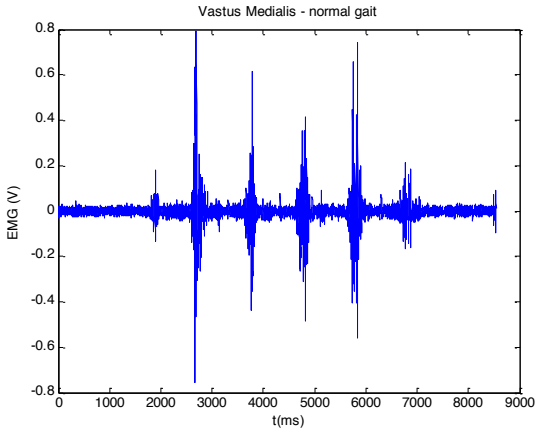

Figure 20 - Typical EMG signal

3.3.9 – EMG processing

The processing of the EMG signal can be made either in the time or in the frequency domain. The objective is always to identify the activation of a given muscle and to estimate the force produced (a hard task as described above). In the time domain it is popular the rectification (absolute value) and the standard deviation or *root mean squared* (RMS) of a moving window of data (Figure 21). Sometimes a moving average (or moving integral) of the rectified signal is also used (green line in the bottom). The root mean square is probably one of the most popular tools (Basmajian and De Luca 1985). This value depends in a complex way on the number of motor units recruited, event duration, anatomy, electric configuration and the characteristics of the instruments.

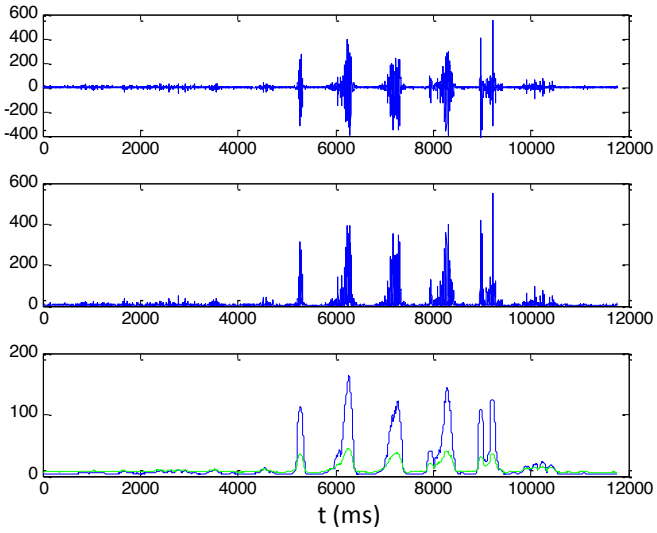

Figure 21 - EMG time processing example

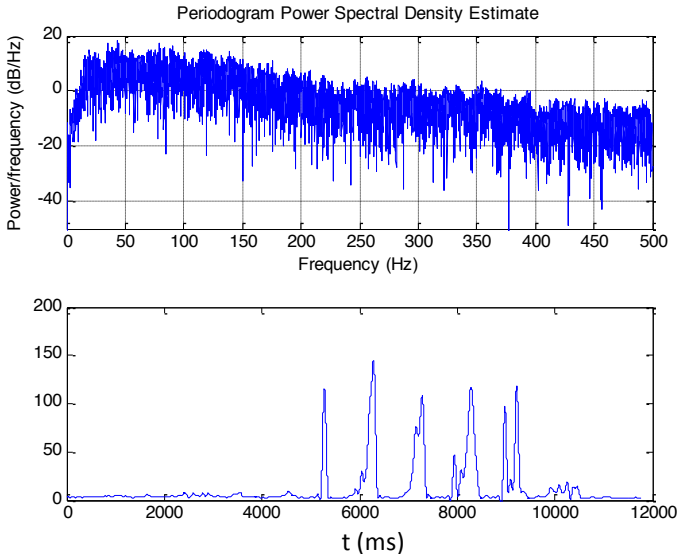

Figure 22 - EMG frequency domain processing example

The frequency domain analysis is most often the signal spectrum estimation and a low-pass filtering to obtain the *envelope* as in Figure 22. The spectrum estimation allows for the detection of signal contamination and also to study fatigue. Fatigue will change the temperature and chemistry (pH) of the muscles and the depolarization/polarization of the fibers becomes slower. Consequently the firing rates become slower and so the average force decreases. The decrease of the depolarization/polarization wave propagation is visible in the 100Hz zone of the spectrum. Also the type II (fast) fibers will fatigue before the type I (slow) ones, making the global intensity smaller. There are algorithms to study fatigue based on a combination of the intensity and spectral content of an EMG signal. Stulen (Stulen and DeLuca 1981) has shown a linear relation between mean and median frequency and the conduction speed of action potentials within muscle fibers.

3.4 – Time-frequency analysis

For some purposes it is interesting to know how the spectral content varies in time. This can be done in a number of ways. The simplest one is to divide the time signal in small sections and compute the spectrum of each one. This is equivalent to a convolution with a squared window and disturbs considerably the spectra. An alternative is to use carefully designed windows, with smooth tails i.e. spectrally less rich that will disturb the signal spectra less. This is the case of the Hamming window that was used to generate Figure 23. However this technique is valid only for stationary signals, what definitely is not the case.

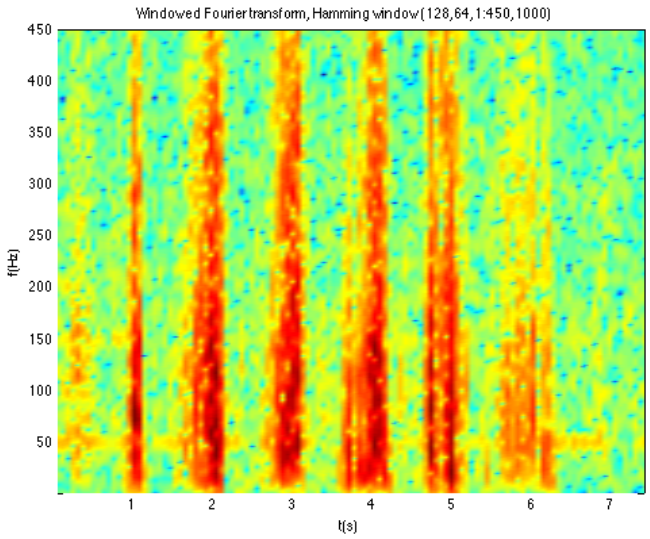

Figure 23 - windowed Fourier transform time-frequency decomposition

An alternative is to implement *windows* or *kernels* that operate both in time and frequency space. Cohen or Wigner distribution functions are used often for that purpose as they are optimal under certain criteria (minimize the time-frequency quantum). Choi-Williams is a Cohen distribution that was used to generate Figure 24. It allows for finer resolution in the time-frequency plane (the kernel is, essentially, the signal, so it is a kind of Fourier transform of the auto convolution).

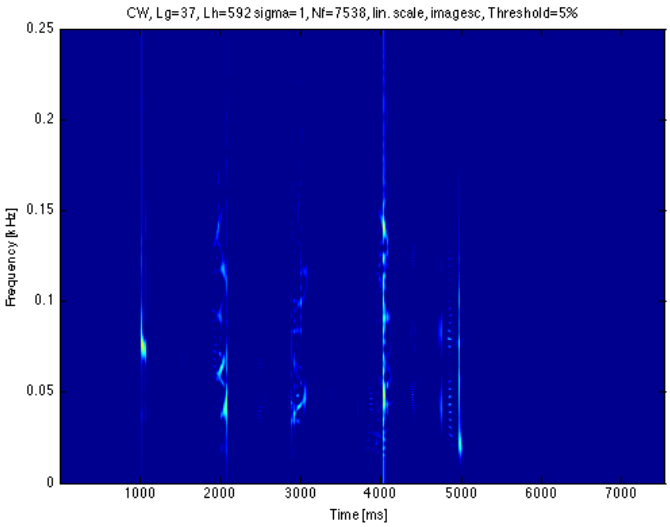

Figure 24 - Choi Williams time-frequency decomposition

Finally we introduce the wavelet transforms. They are resolution adaptative (less time resolved at low frequencies and more time resolved at high frequencies) and are good for transient signals. The idea is to have an L2 space base (the wavelet) that is almost compact both in time and in *frequency*. Then, as in all these decompositions, the signal is projected or decomposed in the elements of that base. We used the Morlet wavelet – a sine wave modulated by a Gaussian – as it has a frequency associated and not just a *scale*. The result is a sort of gaussian windowed Fourier transform but with adaptative resolution Figure 25. Figure 26 is the original time domain signal.

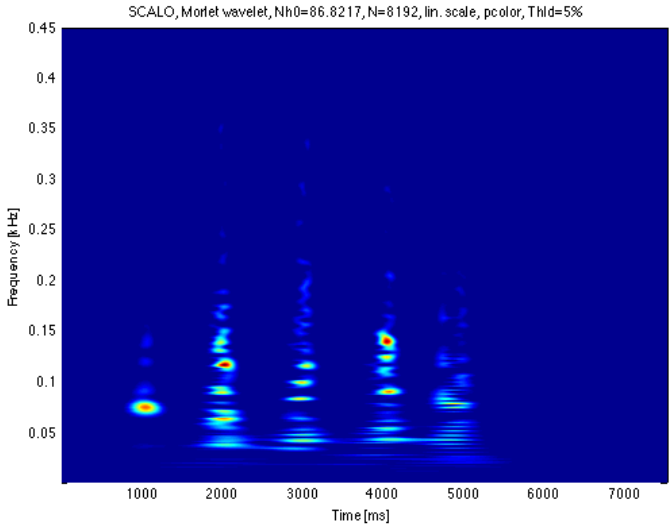

Figure 25 - Morlet wavelet time-frequency decomposition

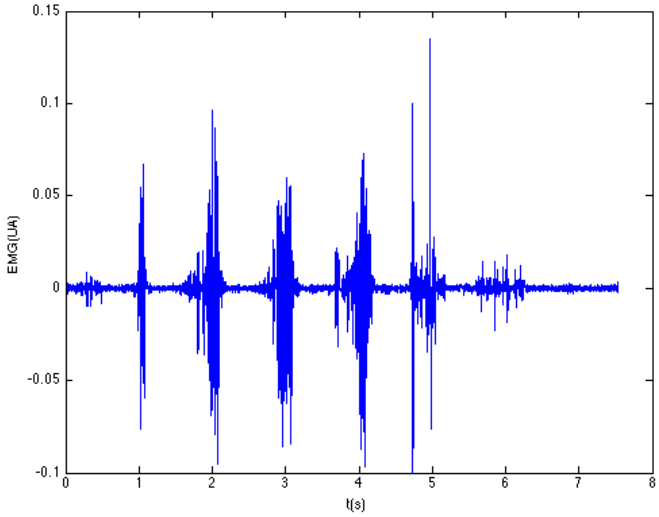

Figure 26 - EMG signal

3.5 – Summary

EMG and force plates are some of the most usual instruments used to evaluate gait. Force plates usually have 6 sensors to measure the three force and torque components. They are composed of amplifiers, filters and an ADC. An EMG is also built with amplifiers, filters and ADC but they can measure electrical currents generated by the muscles. This current is generated by an action potential that polarizes the cell membrane up to +40mV.

A single motoneuron can innervate several muscular fibers of the same type within the same muscle. The force exerted by a muscle is a complex sum of the activation frequencies and the number of recruited fibers. Although the recruitment frequencies are of only a few Hertz the signals wave is spectrally richer than that.

EMG signals can be processed either in time or in the frequency domain. The objective is always to identify the activation of a given muscle and to estimate the force produced. In the time domain it is popular the rectification (absolute value) and the standard deviation or *root mean squared.* Time-frequency analyses are less common and computationally heavier and are made using Fourier transforms or wavelets.

Chapter IV – Development and implementation

4 – Development and implementation

4.1 – Introduction

These codes were devised to aid researchers and clinicians in the analysis of biomechanical signals captured during gait. They return as much information as possible from GRF and EMG data. Although some data analysis was made during the code development phase, in order to verify the calculated outputs, this was not the main objective of this work.

The proposed code for GRF analysis expects two force plate data streams, one for each foot of a stride, and a trigger channel for data cropping and later synchronization with EMG data (at the end a file is written with some synchronization information, to be read by the EMG code). Both GRF and EMG codes were developed independently and can be used almost independently, apart from the mentioned sync file.

Also taken into consideration was the computational cost and run-time of the program. The EMG time-frequency analysis took around 22min per EMG channel with the standard tools on a 2012 top class *wintel* pc. This routine was rewritten and the final code takes just a few seconds on a modern laptop. The time-frequency plots remain, however, very demanding in GPU power.

An effort was made for self containment, so all the functions necessary for this program to run have been written from scratch and stored in independent routines with the exception of the filter implementation and Welch spectrum estimation that requires the signal processing toolbox. This toolbox is usually available on even the most basic Matlab bundles and version 6.11 is even freeware and available on the internet.

The author must also acknowledge that he did not collected any data itself but, for variety, used data provided by different study groups collected at different times with different settings.

In this chapter we will explain how the code is organized the assumptions and optimizations made.

4.2 – Main menu

One of the main concerns during the development of this program was its usability. With that in mind a small menu was created to allow the possibility of choosing one of three actions (Figure 27).

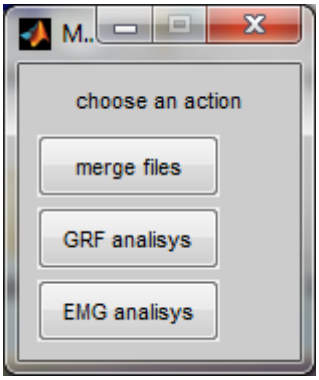

Figure 27 - Main menu

The program allows to choose between EMG/GRF analysis and data fusion. Data fusion (merge files) is an algorithm that will take multiple files from one run and merge all into one file so that the GRF analysis program can evaluate the desired file.

4.3 – GRF data consistency

As a previous step to code development, some empirical choices had to be made. Some data quality analysis was made before data exploration. In several cases the trigger channel was found to have line contamination as can be seen on Figure 28.

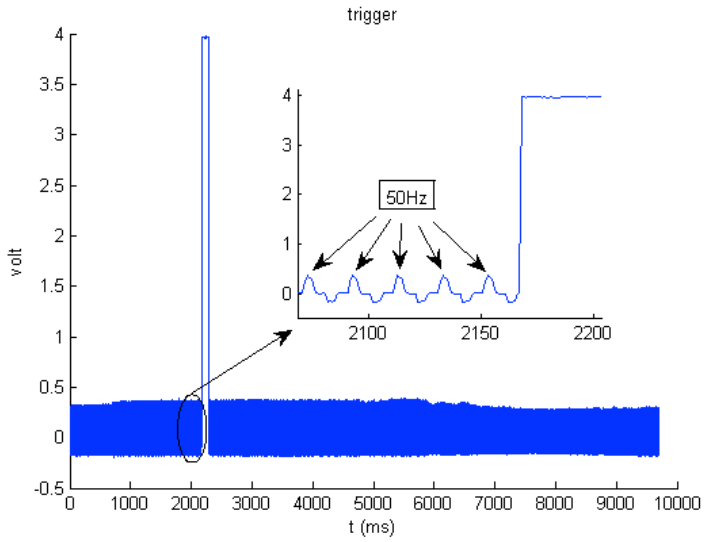

Figure 28 - Trigger channel

This does not interfere with the analysis code, as the TTL trigger logical levels are respected, but the 50Hz noise is probably due to the lack of a pull down resistance in the trigger hardware. Figure 29 represents the trigger probably used in the described experiment and the correction proposed to eliminate the noise.

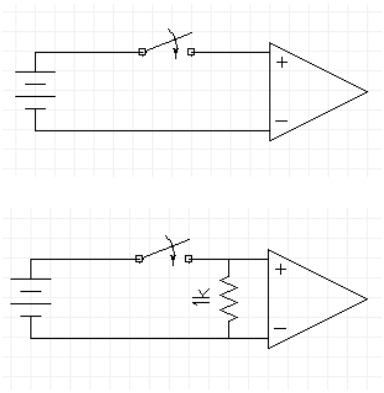

Figure 29 - Trigger and suggested correction

It was also found that in some samples the second platform z-torque channel was disconnected (no data) and was cross-talking with the trigger channel (Figure 30).

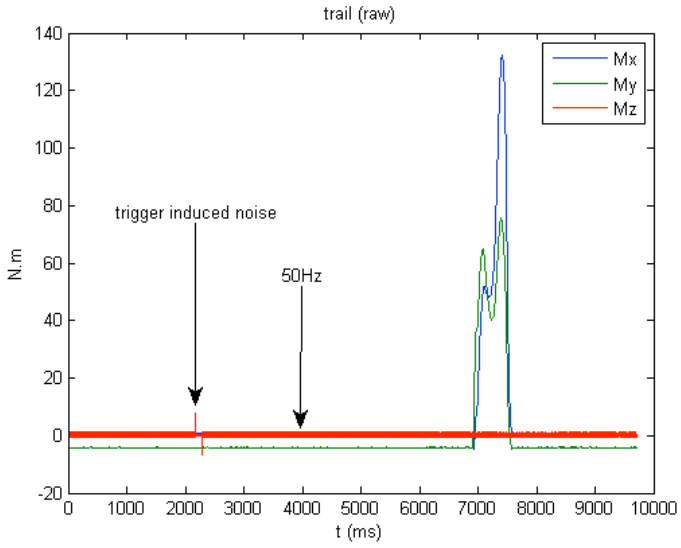

Figure 30 - Second plate z-torque channel cross talking

Fortunately this channel is not used in any computation and therefore no data was rejected.

4.4 – GRF Filter choice

A filtering procedure must only be undertaken if the noise is a clear contaminant of the signal and if it interferes with the analysis. As the noise is never completely known (otherwise it would be easily subtracted from the contaminated signal) filter selection is an empirical procedure that must be carefully taken. For instance (Kirtley 2006) has stated that for the kinematic treatment of a body moving at

the same velocity of our test subjects, a low-pass Butterworth filter with a cut-off frequency of 6Hz is a typical procedure. However we are not dealing with kinematics but dynamics. In a report done by the University of Michigan (Alem and University of Michigan. Transportation Research Institute. 1986) it is stated that the crash-test dummies head sensors should have a cut-off frequency of 550Hz. Many other references quote other values, filters or techniques and so a standard of filtering could not be found.

In this case the data has very little identifiable noise and it will only be used for integration purposes (an operation insensitive to zero-mean stationary noise). Also as stated on chapter 2 the force plates already have built-in filters and are not prone to noise so the type of filters used must be very conservative.

The first problem with the filter implementation is the shift it causes to the signals. For example Figure 31 is a plot of the raw vs filtered data where a 10ms lag can be observed in the Butterworth filtered signal.

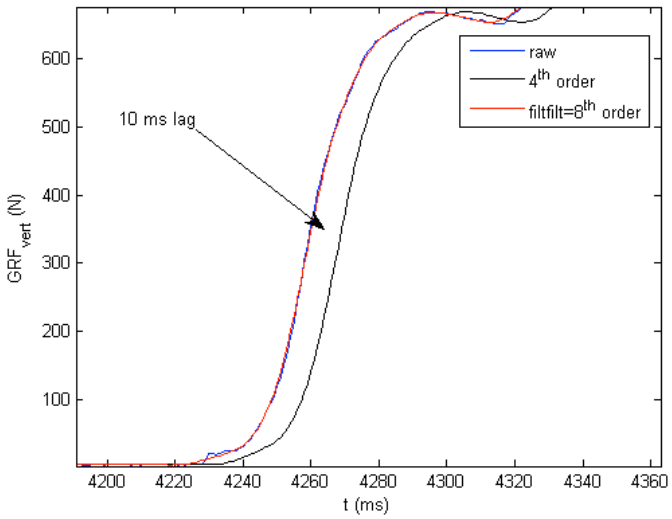

Figure 31 - Raw vs filtered data

To avoid this lag, we can apply the same filter twice, from start to end and then from end to start, effectively creating a double-order zero-lag filter.

The next choice is the type of filter. The standard choice is the Butterworth (IIR) low-pass filter. Figure 32 illustrates its main advantages: it has low undershoot, overshoot and ringing.

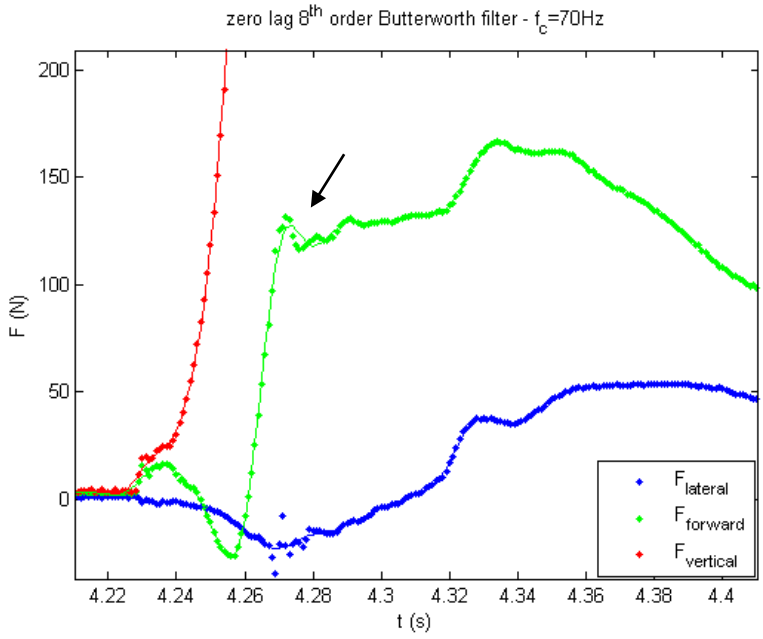

Figure 32 - Force data filtered with a Butterworth

An inspection to the power density spectrum of the force components (Figure 33, Figure 34 and Figure 35) aids at choosing the cutoff frequencies.

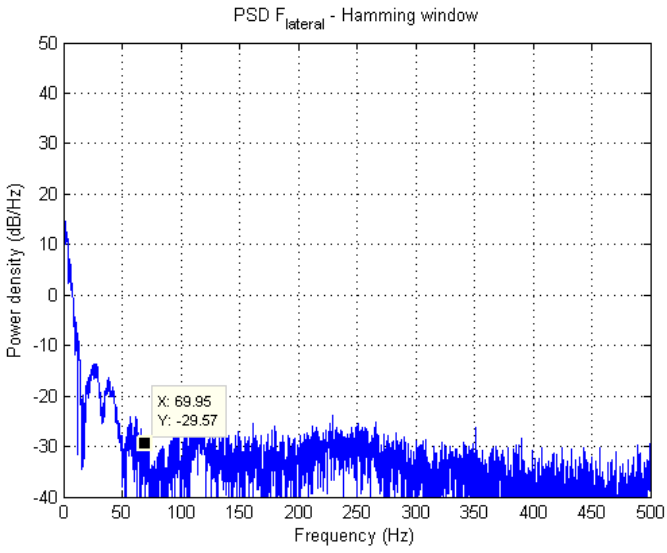

Figure 33 - Power density spectrum of lateral force signal

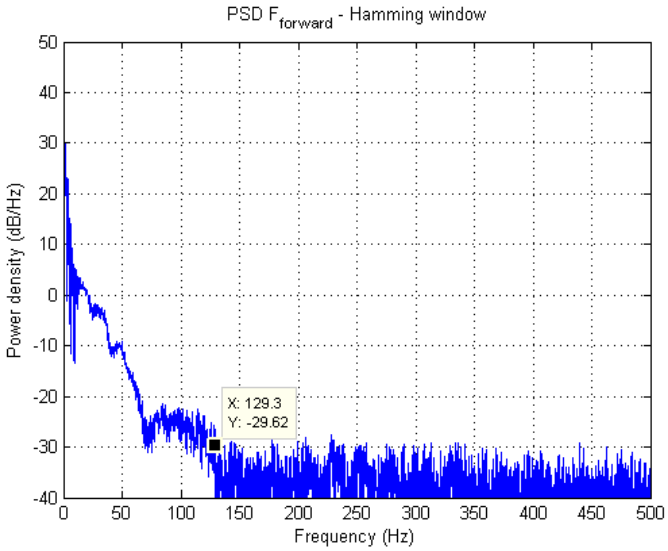

Figure 34 - Power density spectrum of forward force signal

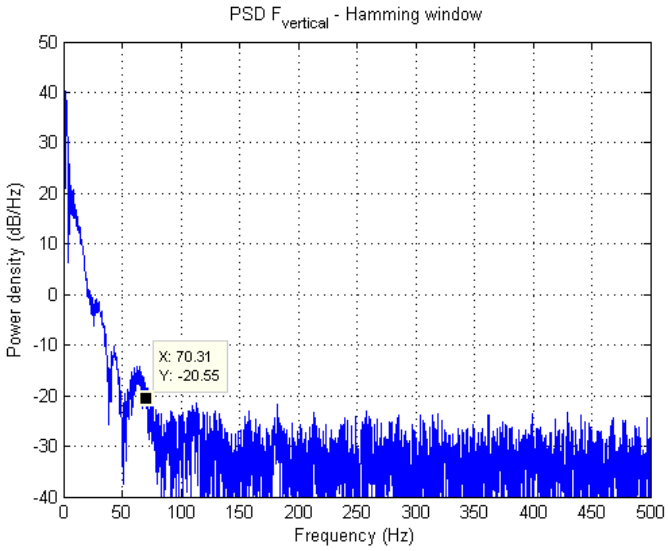

Figure 35 - Power density spectrum of vertical force signal

From this figures we can see a depression in the PSD in the 50Hz band as a result of a notch filter somewhere in the hardware so there's no need to filter this frequency. Also it can be seen that most of the energy of this signals can be found within the 0-70Hz range meaning that to prevent signal loss we should filter only frequencies above 70Hz. Figure 36 and Figure 37 illustrate the importance of a correct cutoff frequency choice.

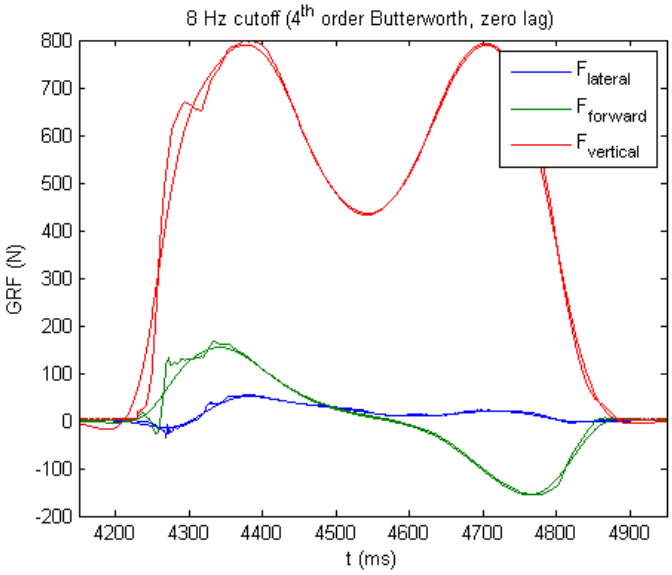

Figure 36 - Raw vs filtered data (8Hz)

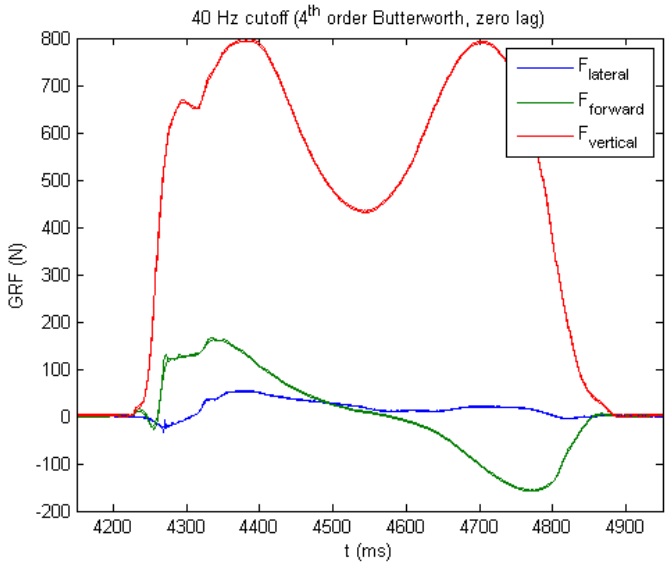

Figure 37 - Raw vs filtered data (70Hz)

From these figures we can see that a cut-off frequency of 8Hz makes the signal lose its characteristics while the 70Hz cut-off frequency maintains the signal pattern and reduces noise. This is important because the GRF analysis made are significantly altered by the filter implementation. For instance with a cut-off frequency of 8Hz the rise time of the vertical and anterior-posterior forces are severely altered as well as all the other calculated parameters as seen in Table **1**.

Table 1 - Error induced by filter with cut-off frequency of 8Hz on one data set

	8Hz	70Hz	Error
trail contact time	0.629	0.606	4%
lead contact time:	0.638	0.619	3%
from trail zero to DA:	0.167	0.181	-8%
DA:	0.116	0.096	21%
from DA to lead zero:	0.195	0.199	-2%
step duration:	0.478	0.476	0%
sride frequency:	2.092	2.101	0%
stride length:	0.633	0.633	0%
Combined Leg Method			
mecanical work from trail zero to DA (+/-):	0	0	
	-36.063	-39.788	-9%
mecanical work DA (+/-):	5.571	4.805	16%
	-12.534	-9.274	35%
mechanical work from DA to lead zero (+/-):	41.762	42.969	-3%
	0	0	
mechanical work over half cycle (+/-):	47.333	47.773	-1%
	-48.597	-49.062	-1%
total mechanical work over half cycle (step):	-1.264	-1.289	-2%
Independent Leg Method			
mecanical work from trail zero to DA (+/-):	0.05	0.089	-44%
	-36.113	-39.876	-9%
mecanical work DA (+/-):	10.717	10.235	5%
	-17.681	-14.704	20%
mechanical work from DA to lead zero (+/-):	41.898	43.006	-3%
	-0.136	-0.038	258%
mechanical work over half cycle (+/-):	52.665	53.33	-1%
	-53.929	-54.618	-1%
total mechanical work over half cycle (step):	-1.264	-1.289	-2%

The duration of the double support is, in this case, wrongly increased by 21% if the wrong cutoff frequency is chosen. This error is of great importance as almost every parameter uses this value as a reference. Although these evaluations here illustrated with one data set the premises are the same for all of them.

Overall, using general rules of thumb and careful inspection of the data and filter effects, we opted to implement an 8^{th} order 70Hz zero-lag lowpass Butterworth filter for GRF data filtering.

4.5 – Step interval calculation

The other empirical parameter is the vertical force level used to determine the beginning and the end of each step. To address this issue a few studies were done to achieve the best compromise. To avoid noise or other signal artifacts to wrongly trigger the contact identification routine and to avoid errors introduced by being overzealous, we opted to define *beginning* when the GRF surpasses 1% of the body weight and maintains this for at least 50ms. This is also used to determine the end of each step, reversing the condition. Figure 38 and Figure 39 shows the difference when using a 7% criteria and a 1% criteria as the threshold.

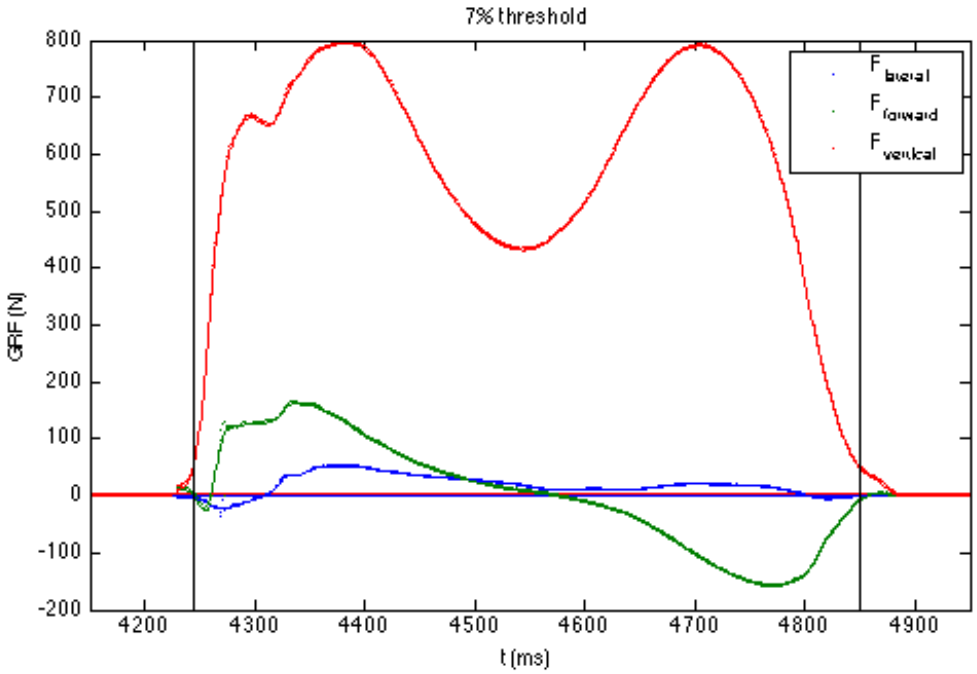

Figure 38 - Step start and end calculation using 7% body weight as threshold

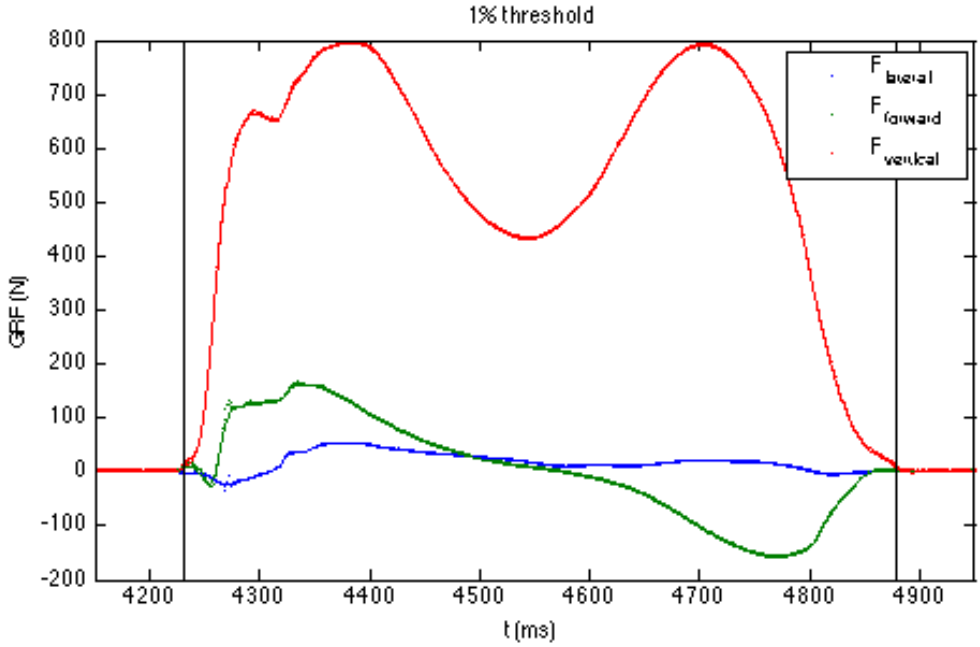

Figure 39 - Step start and end calculation using 1% body weight as threshold

It can be seen from the figures above that 1% body weight along with the 50ms contact time is enough to correctly determine the step beginning and ending. Once again these parameters must be correct in order for the calculated quantities to be correct as all of them depend on the correct calculation of all time intervals. Table 2 shows the amount of error made on all the calculated values as a result of an incorrect choice of threshold.

Table 2 - Error induced by an incorrect choice of threshold

	7%	1%	Error
trail contact time	0.606	0.649	-7%
lead contact time:	0.619	0.655	-5%
from trail zero to DA:	0.181	0.171	6%
DA:	0.096	0.135	-29%
from DA to lead zero:	0.199	0.17	17%
step duration:	0.476	0.476	0%
sride frequency:	2.101	2.101	0%
stride length:	0.633	0.633	0%
Combined Leg Method			
mecanical work from trail zero to DA (+/-):	0	0	0%
	-39.788	-37.06	7%
mecanical work DA (+/-):	4.805	12.054	-60%
	-9.274	-12.002	-23%
mechanical work from DA to lead zero (+/-):	42.969	35.72	20%

	0	0	0%
mechanical work over half cycle (+/-):	47.773	47.773	0%
	-49.062	-49.062	0%
total mechanical work over half cycle (step):	-1.289	-1.289	0%
Independent Leg Method			
mecanical work from trail zero to DA (+/-):	0.089	0.041	117%
	-39.876	-37.1	7%
mecanical work DA (+/-):	10.235	17.553	-42%
	-14.704	-17.502	-16%
mechanical work from DA to lead zero (+/-):	43.006	35.736	20%
	-0.038	-0.016	138%
mechanical work over half cycle (+/-):	53.33	53.33	0%
	-54.618	-54.618	0%
total mechanical work over half cycle (step):	-1.289	-1.289	0%

4.6 – GRF processing

The GRF processing code has an easy to use and easy to read interface that allows the analysis of GRF data if some conditions are meet. The data must be collected from a set of 2 force plates (one for each foot) and no more than one contact by platform can be made. The data must be in a single file containing the two force plates forces and moments as well as the trigger channel. If the force plate and trigger data are in two or more separate files or if the file has a header then it must be pre-processed by user codes. Also if data is floating point it must have a decimal point as separator (new matlab versions might read also the Portuguese comma decimal symbol). All the necessary input is asked prior to any other action. The implemented algorithm is divided in several sub-routines for better readability. We shall analyze and explain it one by one. Figure 40 is a schematic representation of the code.

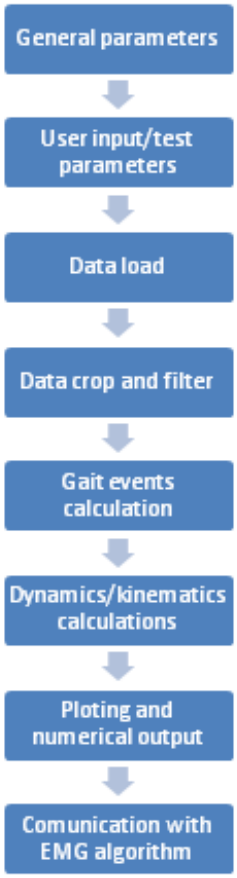

Figure 40 - Algorithm schematics

The first thing the program does is to clear and close everything that matlab is doing. This helps to keep a clean look and also makes it quicker to run. General parameters are a set of pre-defined variables within the code that almost never change (gravity acceleration, etc). It's then followed by the user input parameters that are a set of variables that can change from test to test (sampling rate, data channels in the files, etc). In *data load* the user selects the data he wants to analyze and it's then cropped and filtered. Gait events such as step start and stop are then calculated for the dynamic/kinematic evaluation. The program then returns several plots and numerical outputs as well as a file with the gait events that are used in the EMG analysis.

4.7 – General and test parameters

General parameters are a pre set of variables that can be changed but do not appear in the user interface because usually, for most of the studies, they are kept

unchanged. Those variables are the window (in seconds) used to average the offset, the minimum time above threshold to validate an event, the cut-off frequency of the low-pass Butterworth filter, half the order of the filter, the body weight percentage to use as trigger and the gravity acceleration. If necessary they can be easily changed in the matlab script.

The test parameters usually change depending on whose leading the experiment or the way the data is stored. Once the program is running a dialog box will appear (Figure 41) and all the test parameters can be filled.

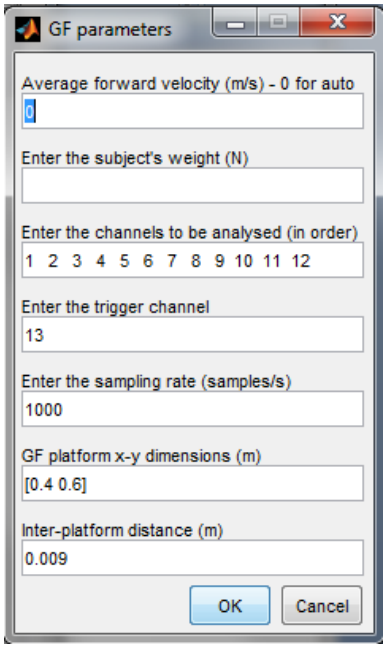

Figure 41 - Input dialog

The average forward velocity can be automatically calculated from the COM displacement so usually there's no need for changing this. However the choice of using the velocity calculated by the algorithm or one measured by cinematic or radar is offered. By default it is calculated automatically. The subjects' weight is something that changes every time a new subject is analyzed so makes perfect sense to be able to change it every time we run the program. Probably the most complicated input parameter are the channels to be analyzed. The channels must have the following order [Fx1, Fy1, Fz1, Mx1, My1, Mz1, Fx2, Fy2, Fz2, Mx2, My2, Mz2]. Then the trigger channel must be introduced. The frame rate, plate size and inter-plate distance can also be changed if the experimental layout and force plates used changes (usually when researching in other facilities). Figure 41 illustrates this interface. Embedded in the code is an input check that verifies the submitted values and fails if any of them is incorrect.

4.8 – Data load, crop and filter

After all the settings are chosen is then necessary to select the data we want to analyze. A window will appear (Figure 42) to choose the data file to be analyzed.

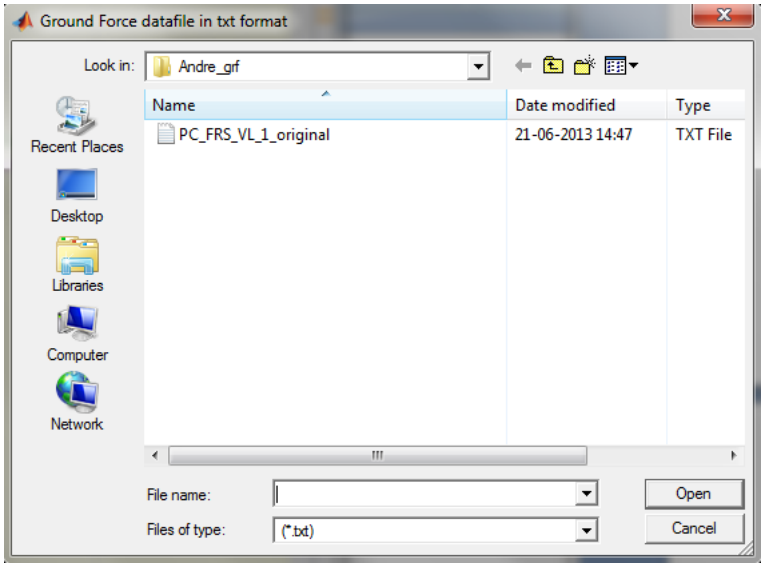

Figure 42 - Data file selection

Txt is the predefined file format for this program but it will also accept other file formats such as xls, cvs and matlab. After the file selection all channels will be cropped and aligned according to the trigger position. The trigger event is calculated using a function called *inicio* created to find the first point that stays above the threshold for at least dt seconds. Both the threshold and dt values have been chosen to deal with the typical trigger values. As the trigger is TTL like, the threshold was 2.5V with a dt of 50ms. The data is then filtered as stated above and finally the remaining DC component is removed by subtraction with the average of the first 0.5s of each data channel.

4.9 – Gait events

The gait events are the start, stop and zero forward force step instants. These events divide the gait into well delimited actions as shown in Figure 43. To calculate these events three sub-routines were designed *inicio, zero_cross* and *fim*. The first one was already explained above, the last one is the same as *inicio* but does it from the end to the beginning of the time series.

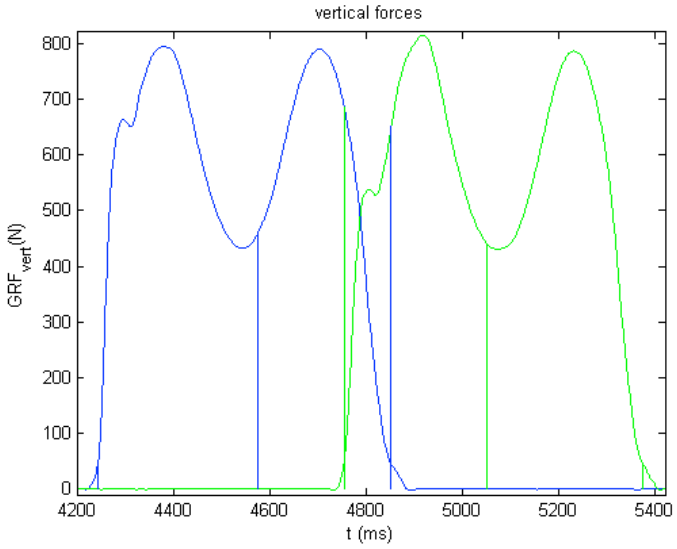

Figure 43 - Gait events (vertical forces)

This way one calculates the starting points and the other one the ending points. The *zero_cross* function calculates the instant where the forward force is null (ignoring inertial effects, this is a consequence of COM being vertically aligned with the COP). In case of an abnormal force pattern this function will find the middle zero crossing point (odd number of crossings) or the first after the middle (even number of crossings). We can now calculate all the time intervals such as the trail, lead and the double support contact times by subtracting those instants.

4.10 – Dynamics

The algorithm first calculates the COP location as shown in equation 1. It also adds the inter plate distance to the COPy.

$$\overrightarrow{COP} = \frac{\vec{M}}{F_z}$$

Equation 1 - COP position

From the COP data we can now know the horizontal displacement and the COM average velocity but only within the two zeros interval (Figure 44). That's because it's the only cycle (step) were all the forces are known and therefore where all the COM related calculations can be made. The COM trajectory can also be determined (if the subject is symmetric) but this will be discussed further ahead.

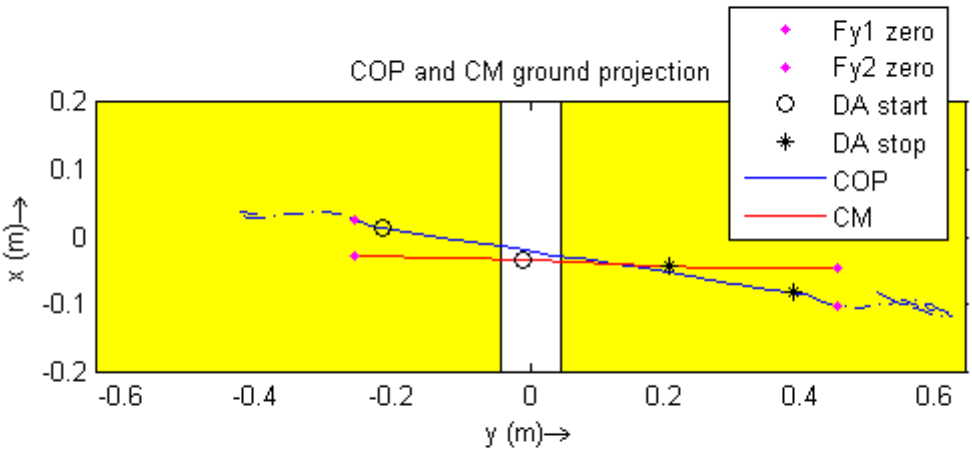

Figure 44 - COP and COM trajectory

It is now easy to calculate which is the first leg simply by watching at the lateral displacement. If COPx(zero1) < COPx(zero2) then the first leg is the right one. The average forward COM velocity can also be calculated from the COP for the zero1:zero2 interval because on the zero points the COM should be above COP. The average vertical velocity is considered zero otherwise the subjects would be either falling down or rising up. The initial and final lateral velocity (zero1:zero2) is also considered to be zero. This may not be true to very asymmetric subjects. The COM velocity variation can also be calculated using the equation 2:

$$\overrightarrow{\Delta V} = \int_{zero1}^{zero2} \left(\frac{\overrightarrow{F_1} + \overrightarrow{F_2}}{m} - \vec{g} \right) dt$$

Equation 2 - Velocity variation

To calculate the defined integral a small function was written to calculate integrals by the Simpson's extended rule with four endpoints. We can now calculate the initial velocities (equation 3):

$$\overrightarrow{V_0} = \langle \vec{V} \rangle - \overrightarrow{\Delta V}$$

Equation 3 - Initial velocity

And the instantaneous velocity as well (equation 4 and Figure 45):

$$\vec{V}(t) = \overrightarrow{V_0} + \overrightarrow{\Delta V}$$

Equation 4 - Instantaneous velocity calculation

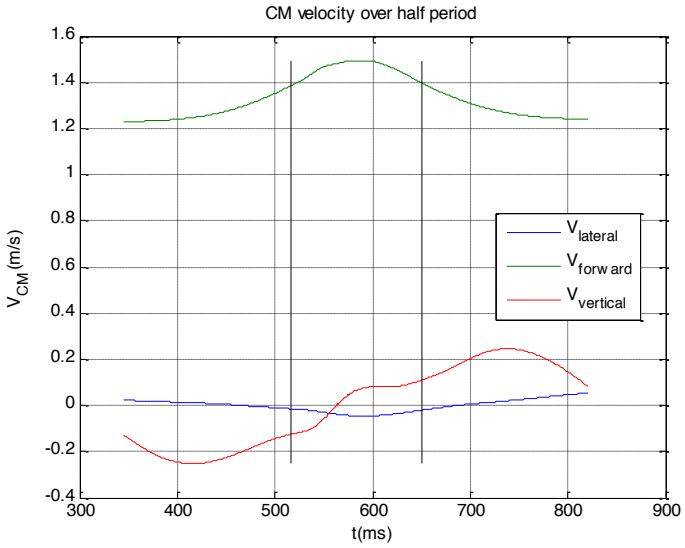

Figure 45 - Instantaneous velocity of COM

We can also calculate the stride velocity variation by applying the equation 1 for the stride interval (start1:stop2). The COM displacement can be calculated by further integrating the forward and vertical velocities for the zero1:zero2 interval (equation 5).

$$\vec{r}_{COM}(t) = \int_{zero1}^{t} \vec{V}(t)\, dt + \vec{C}$$

Equation 5 - COM position calculation

The $\vec{C}$ constant is the position of COM at a given time instant. Ignoring the small *inertial forces*, at zero1 the COM will be above COP in the Y axis thus making C_y(zero1) = COP_y(zero1). For the lateral COM position we have stated that for the middle of the DA phase COM_x will be located at the COP_x position, C_x(<DA1:DA2>) = COP_y(<DA1:DA2>). Because C_z cannot be calculated only the horizontal trajectories can be traced (Figure 44). Figure 46 shows the COM_z displacement.

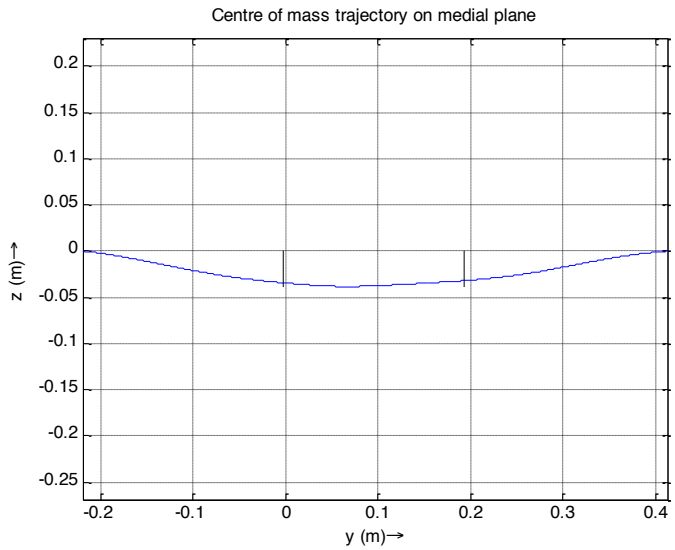

Figure 46 - COM vertical displacement

By plotting the COP vs COM forward trajectory we can observe the relative positions of COM and COP, and evaluate the reusage of energy (Figure 47).

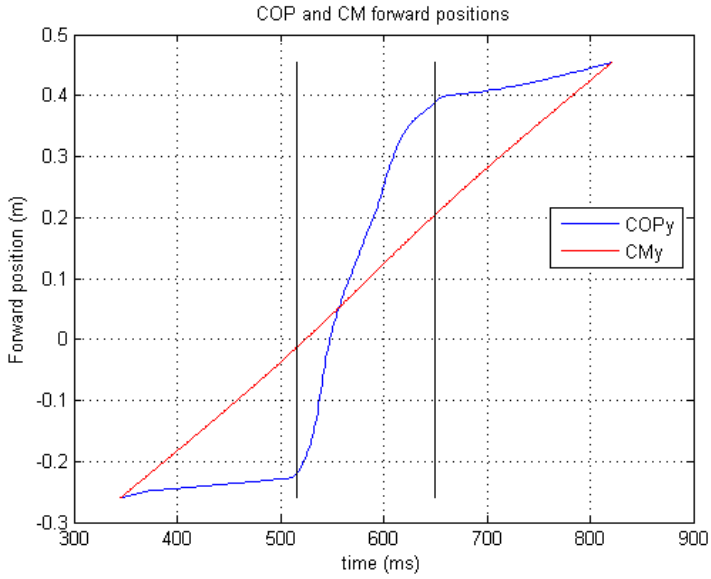

Figure 47 - COM vs COP forward position

Power calculation is made for both the individual limb and combined limb methods. The ILM calculates power individually for both legs and CLM doesn't (equation 6).

$$P_{Lead/Trail} = \overrightarrow{F_{Lead/Trail}} \times \overrightarrow{V_{COM}}$$

$$P_{CLM} = \overrightarrow{F_{tot}} \times \overrightarrow{V_{COM}}$$

Equation 6 - Power calculation for ILM and CLM

The work is calculated by time integration equation 7

$$W_{trail} = \int_{POS/NEG} P_{trail}\, dt$$

$$W_{CLM} = \int_{POS/NEG} P_{CLM}\, dt$$

Equation 7 - positive and negative work calculation for each method

In Figure 48 we can see the power generated on the body's COM

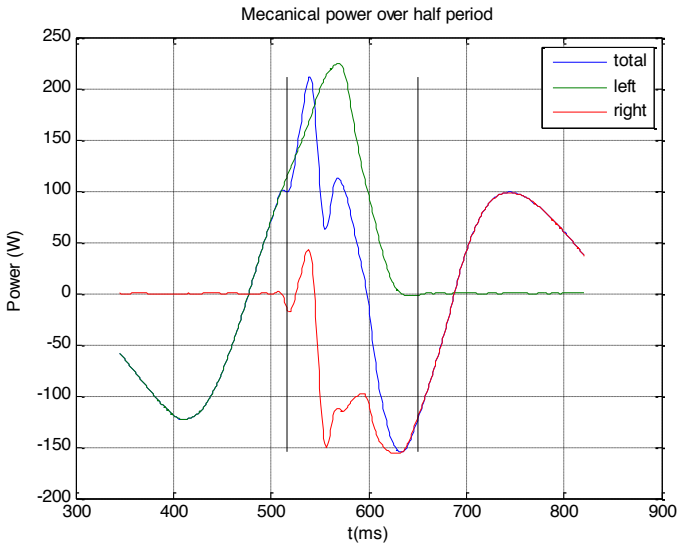

Figure 48 - Power during one cycle

4.11 – Plotting and numeric output

This part of the code is responsible for showing the results calculated above. An effort was made to present the results in the clearest way possible (Figure 49). All units

are on the SI system (with the exception of time in some plots). Besides the numerical output the program also plots all figures that can aid in the understanding of the results (Figure 44 to Figure 48).

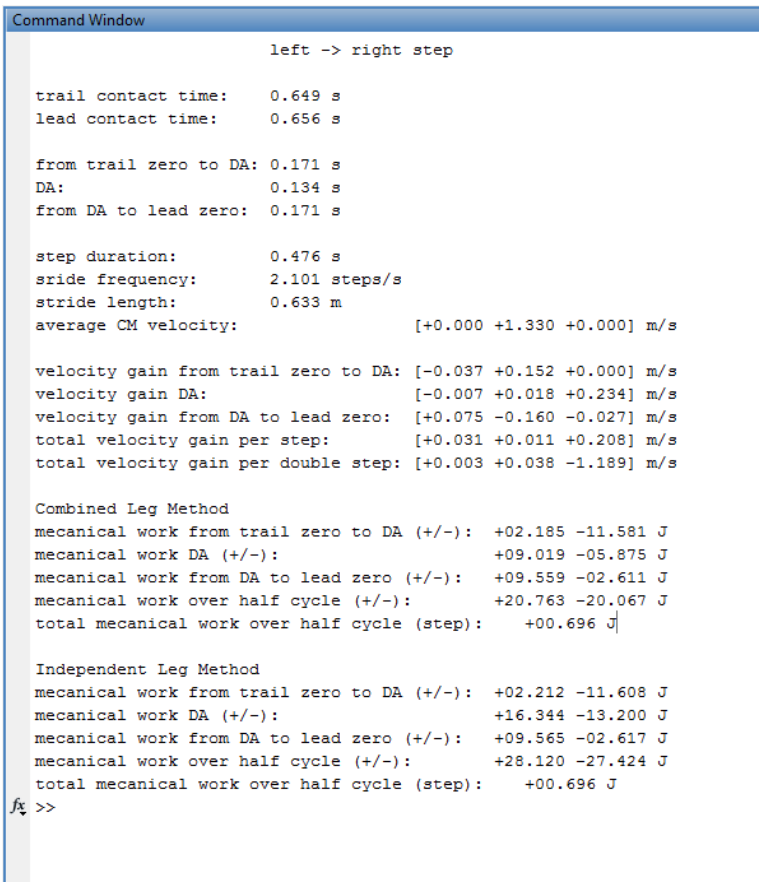

Figure 49 - Numerical output

The final part of the algorithm stores several variables of interest in a matlab file so they can be available for the EMG processing algorithm.

Another file, incremental, will record a much richer output of each analysis for post-processing.

4.12 – EMG filter choice

The EMG signal was studied to better understand the need to filter it or not. A PSD analysis was made for the raw signal and another one for the signal filtered with a Butterworth band-pass filter with a pass-band of 20-450Hz (Figure 50). It was found that the hardware, as expected, had already filtered the signal with a 20Hz high-pass and an anti-aliasing filter. The implementation of another filter would only cause signal loss and it's not advisable at all.

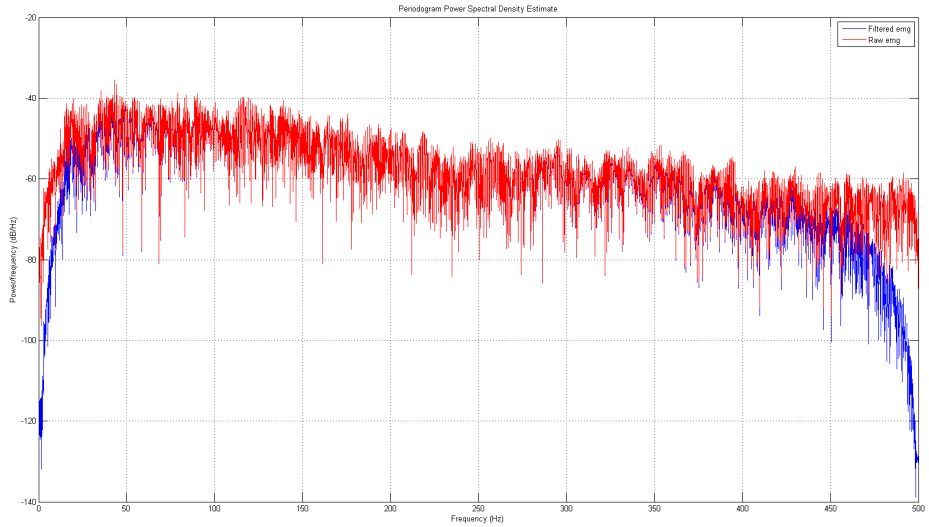

Figure 50 - PSD of raw and filtered EMG data

4.13 – EMG algorithm implementation

The algorithm structure is very similar to the GRF analysis in the first steps as seen on Figure 51. The program has a set of pre-established parameters that can be changed, if necessary, within the script. Usually these parameters do not change from study to study. All the inputs that can change easily due to the experimental conditions can be changed in the user input dialog box (Figure 52). This input box was created to be as simple to use as possible. Some of the inputs needed are the channels to be analyzed as well as the trigger channel. Also it gives the user the possibility to implement a Butterworth pass-band filter in the 20-450Hz range or a 50Hz notch filter and to make and see the time-frequency analysis.

Data load is made in the same way as in the GRF algorithm. A window will appear to choose the two data files to be analyzed (one for each leg). The program also finds the data rate and resolution used during data acquisition by looking at the files headers. All these inputs are checked for any incorrect values and an error will appear if so.

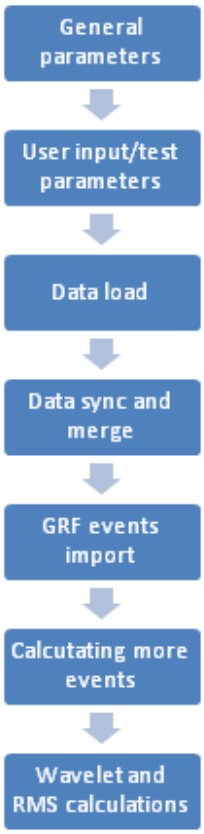

Figure 51 - EMG algorthm schematics

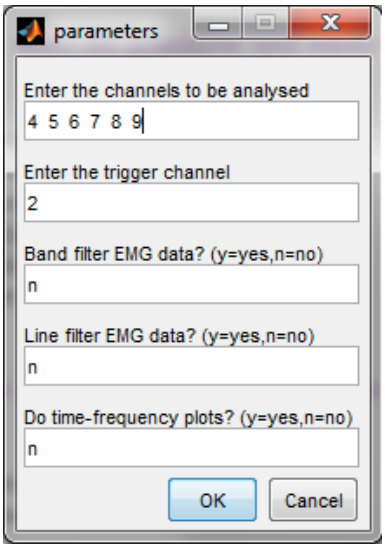

Figure 52 - EMG input dialog

The data is then synchronized using as reference the trigger event. Because some files have different trigger policies it is used the same routine built on the GRF algorithm to find the trigger event. It will find the first point that crosses the threshold value and stays there for at least 50ms (this value can be changed in the general parameters section). The trigger channel is then discarded and all the selected data channels merged into one matrix.

Prior to any calculations the data offset is removed by subtracting the average value of the first 0.5s of each channel and the scaling is also adjusted. The variables calculated in the GRF analysis program are imported and converted to the correct time (in case data rate differs for both signals). Four more time instants are added corresponding to the 2 peaks in each vertical GRF signals. This is done to further increase the number of gait intervals (Figure 53). This has no influence on the calculations made further ahead and is done only to better understand which muscles are working at the different intervals.

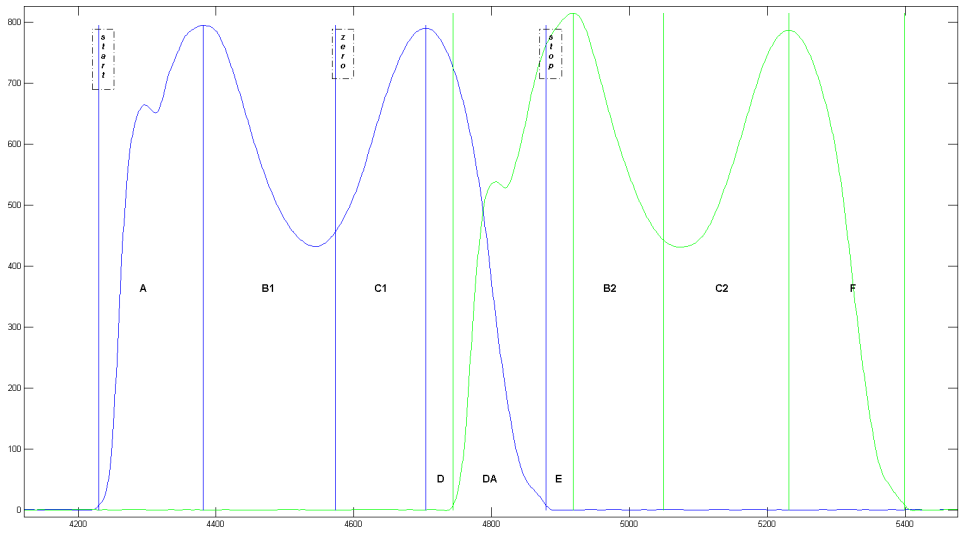

Figure 53 - Gait intervals

4.14 – EMG wavelets and RMS calculation

This is the most important part of the processing algorithm. It calculates the RMS for every interval and the signal envelope as seen on equation 8. The standard definition is

$$RMS_k = \sqrt{\frac{\sum_{i=k-n/2}^{k+n/2} EMG_i^2}{n}}$$

Equation 8 - Envelope calculation

However, in order to properly address the boundaries and for efficiency reasons this is implemented as a convolution (equation 9) with a squared window of unitary amplitude and width *n*.

$$\boldsymbol{RMS_k = \sqrt{\frac{EMG^2 \circledast window(k,n)}{n}}}$$

Equation 9 - Envelope calculation

where $\circledast$ is the convolution operator and $\boldsymbol{window(k,n)}$ is the window with centre in k and width n.

Once all calculations are done the program returns a plot for each channel with the EMG signal, envelope and all the originally calculated gait events (starts, stops and zeros) as seen on Figure 54

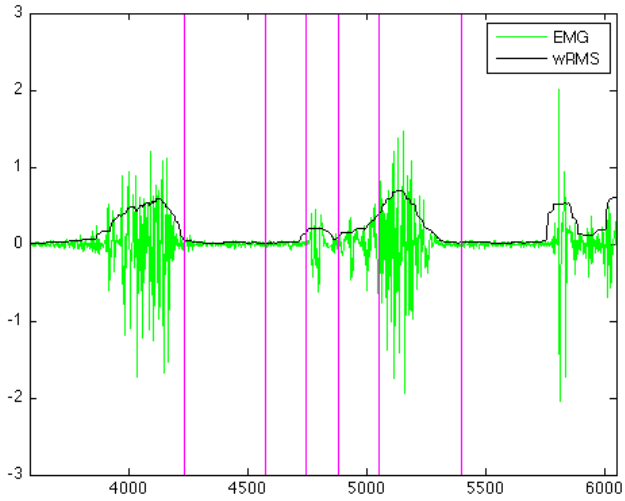

Figure 54 - EMG analysis plot output

The numerical output is presented on the matlab console and is the result of the RMS calculations for every interval. The output is very clean and easy to read. Every column represents a time interval and every row a muscle (Figure 55).

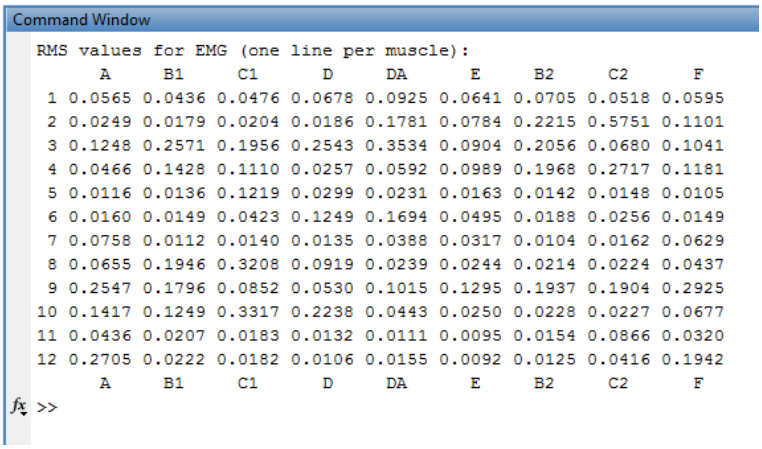

Figure 55 - EMG numeric output

4.15 – Calculating activation patterns

The program offers the possibility to make a wavelet analysis of the EMG signals. This type of analysis uses a Morlet wave to calculate the frequencies present on the EMG. This is a very time consuming and heavy on the RAM and CPU process. Originally the wavelet analysis program was part of a free toolbox (Auger, Flandrin et al. 1995-1996) and would take more than 20 minutes for each EMG channel analysis. The code was changed to be independent and faster. Among the speed related changes are the use of FFT based convolutions (instead of the definition based matlab routine *conv*) and the zero padding to achieve a power of two lengths as the FFT works faster this way. These changes made the code more than ten times faster. Also some reordering of the instructions and general memory access optimization provided similar gains. The reduction on the number of *voices* used to 1024 reduces computation time even more. Some optimizations on the Hilbert analytical representation were also done, avoiding one FFT in the convolution process. After optimization each EMG analysis takes no more than a few seconds (depending on data length).

The code can generate two types of plots. One is the time-frequency decomposition by wavelet analysis and the other correlates the EMG and envelope with the mean and modal frequencies (Figure 56).

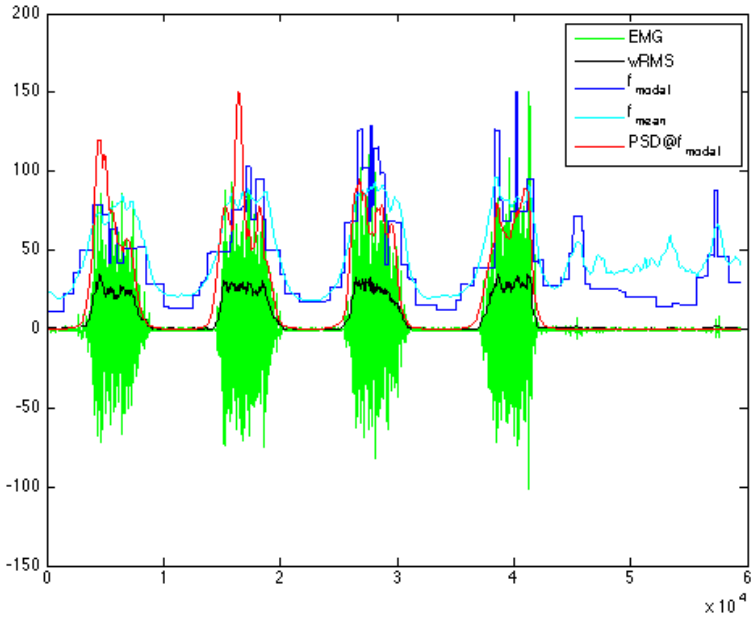

Figure 56 - Combined plot of EMG wavelets analysis

During the development of this algorithm it was found that the modal frequency appears to be a good indicator of muscular activation as seen on the Figure 56. To the best of our knowledge (and if proven usefull) this would be a completely new way of determining muscular activation.

Due to time limitations, up to date, no conclusive studies were made to verify the authenticity of this claim. An experiment with a single subject was made to study this hypothesis but the results were not conclusive. The experimental protocol consisted of four runs, each one with four different types of isometric contractions, slow and sub-maximum, slow and maximum, fast and sub-maximum and fast and maximum. The objective was to study the effect of different types of muscular contractions on activation patterns determination. A force plate was used alongside the EMG to confirm force production and to study the possibility to predict muscular pre-activation. By order Figure 57 to Figure 60 are the results of those studies.

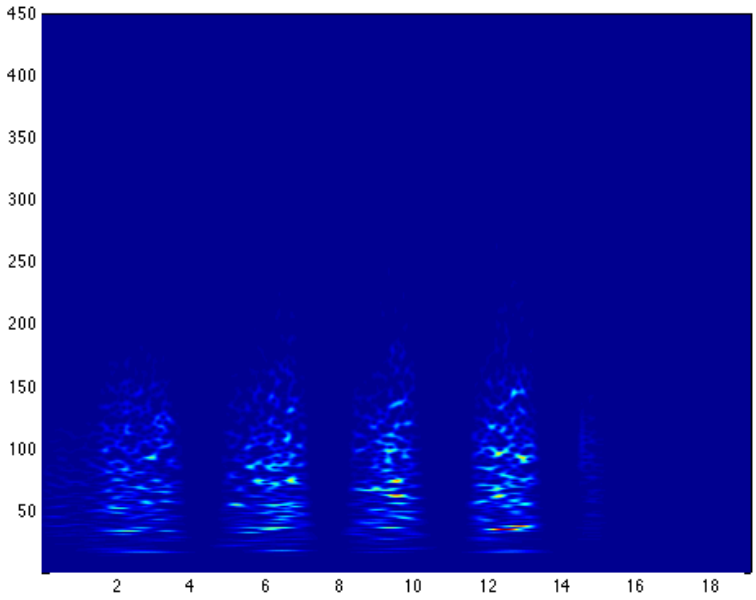

Figure 57 - EMG wavelet analysis for slow sub-maximum contraction

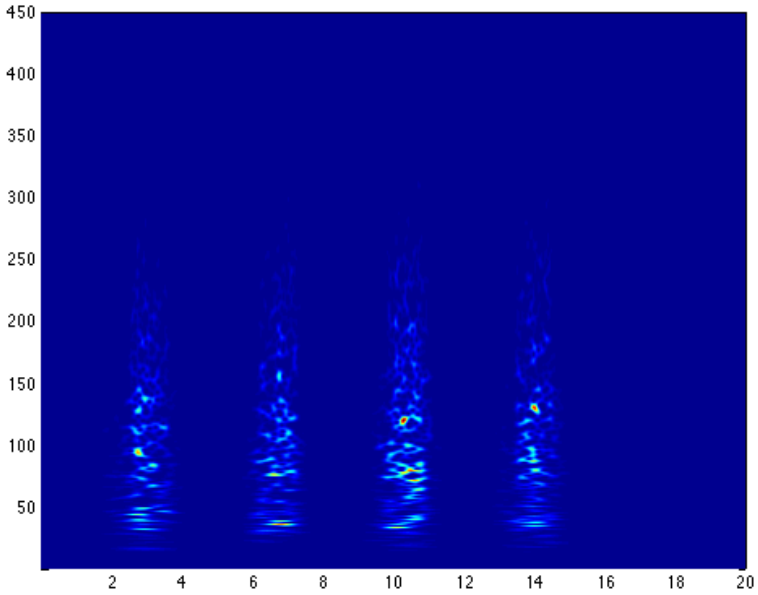

Figure 58 - EMG wavelet analysis for slow maximum contraction

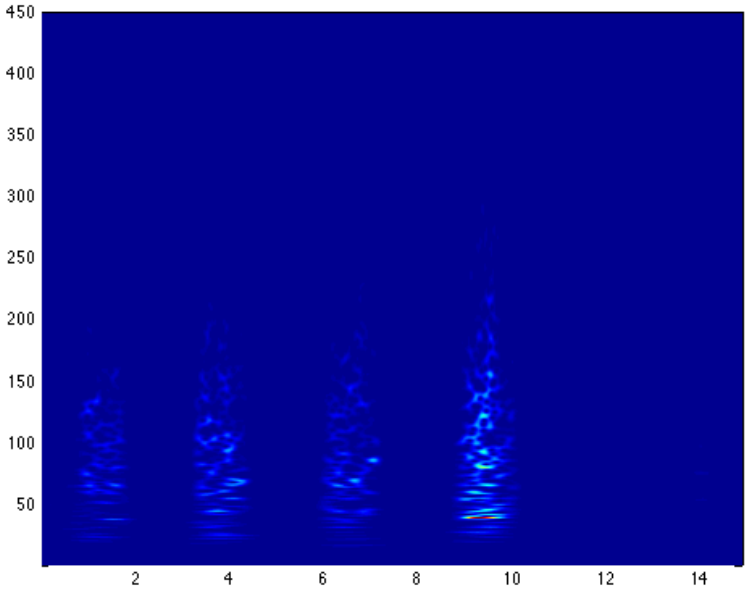

Figure 59 - EMG wavelet analysis for fast sub-maximum contraction

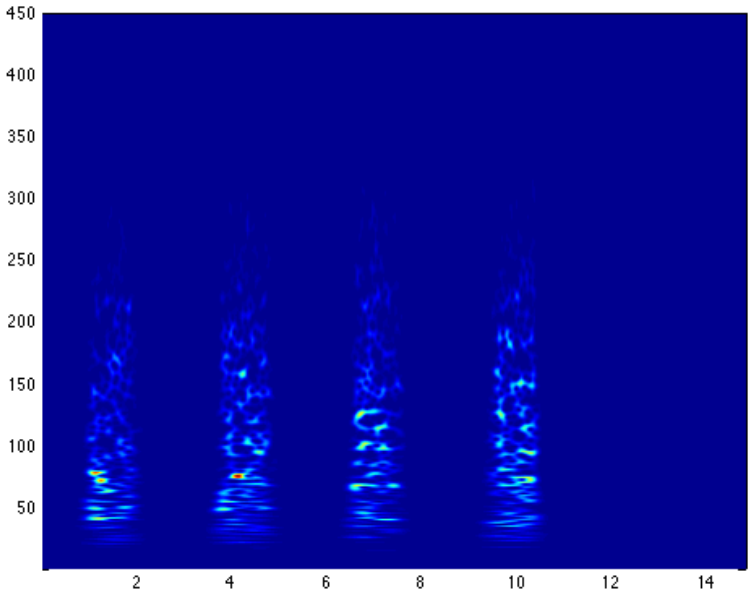

Figure 60 - EMG wavelet analysis for fast maximum contraction

From this figures it is clear to see the diverse recruitment frequencies of each motor unit. We can also observe the intricate pattern of muscular activation and an apparent increase in activation frequencies with the force increase. When overlapping the modal and mean frequencies of each test to the EMG signal we get the Figure 61 to Figure 64.

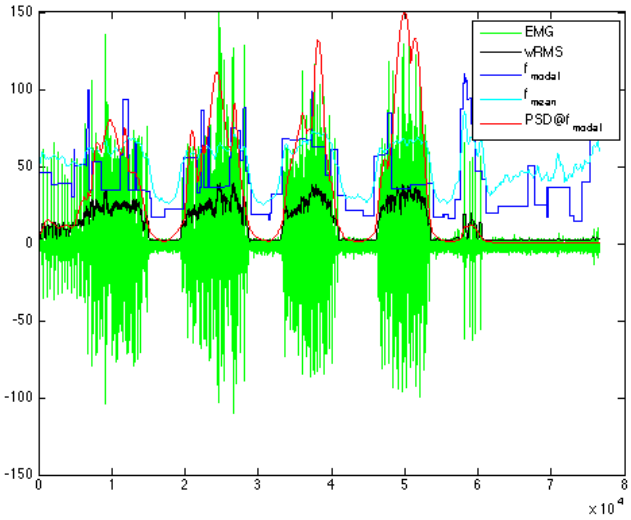

Figure 61 - Combined plot of EMG wavelets analysis slow sub-maximum contraction

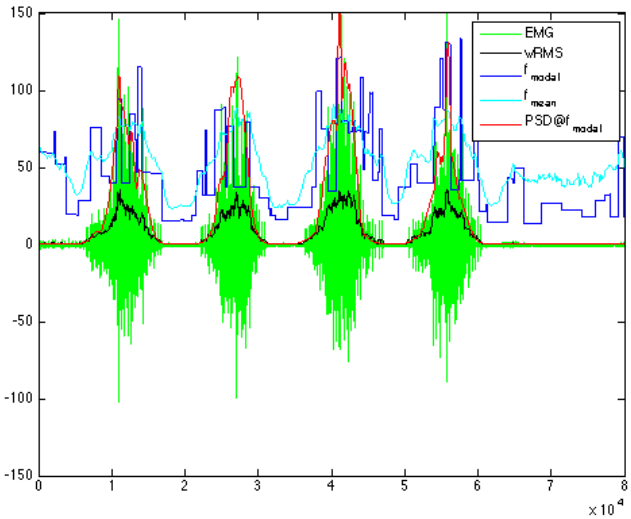

Figure 62 - Combined plot of EMG wavelets analysis slow maximum contraction

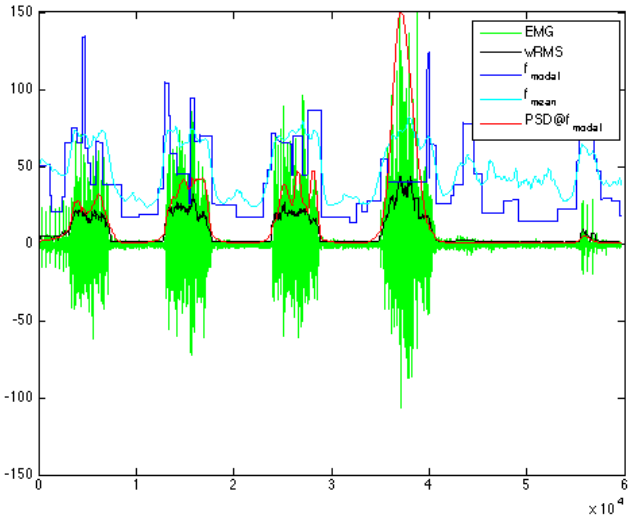

Figure 63 - Combined plot of EMG wavelets analysis fast sub-maximum contraction

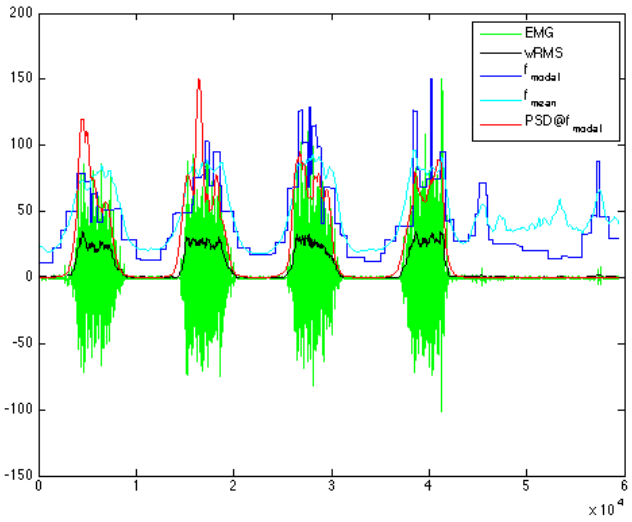

Figure 64 - Combined plot of EMG wavelets analysis fast maximum contraction

From these figures is not completely clear that the modal frequency is a predictor of muscular activation and more tests need to done. On these grounds we do not advise the use of this technique until further studies are made and no implementation based on this is provided.

4.16 – Summary

A lot of work was spent to study the basic assumptions. All the filters, thresholds and cut-off frequencies were analyzed to suit the needs best. The code is organized in a practical easy-to-use graphical interface and it is composed of three main blocks. The merge files program takes several files from the force plates and merges them into one so it can be analyzed. The GRF analysis takes merged GRF files and calculates COP and COM displacements, velocities, impulse and work. It will also store some of the calculated variables into a file for the EMG analysis. The EMG analysis program does an RMS and wavelet calculation.

A new technique is also suggested to calculate activation times based on the frequencies. More studies are needed to evaluate this technique but the results look promising.

Chapter V – Results

5.1 – Introduction

5.2 – GRF results

5.3 – EMG results

5.4 – Summary

5 – Results

5.1 – Introduction

The current chapter focuses on the obtained results calculated by the program and its analysis. We will evaluate the gait of a normal and an impaired subject. We will also analyze a multi-step-per-plate run.

All the graphical and console outputs for both the GRF and EMG analysis program will be shown.

5.2 – GRF results

The GRF analysis algorithm has been tested with several subjects both normal and impaired. These are the results for a normal gait (Figure 65).

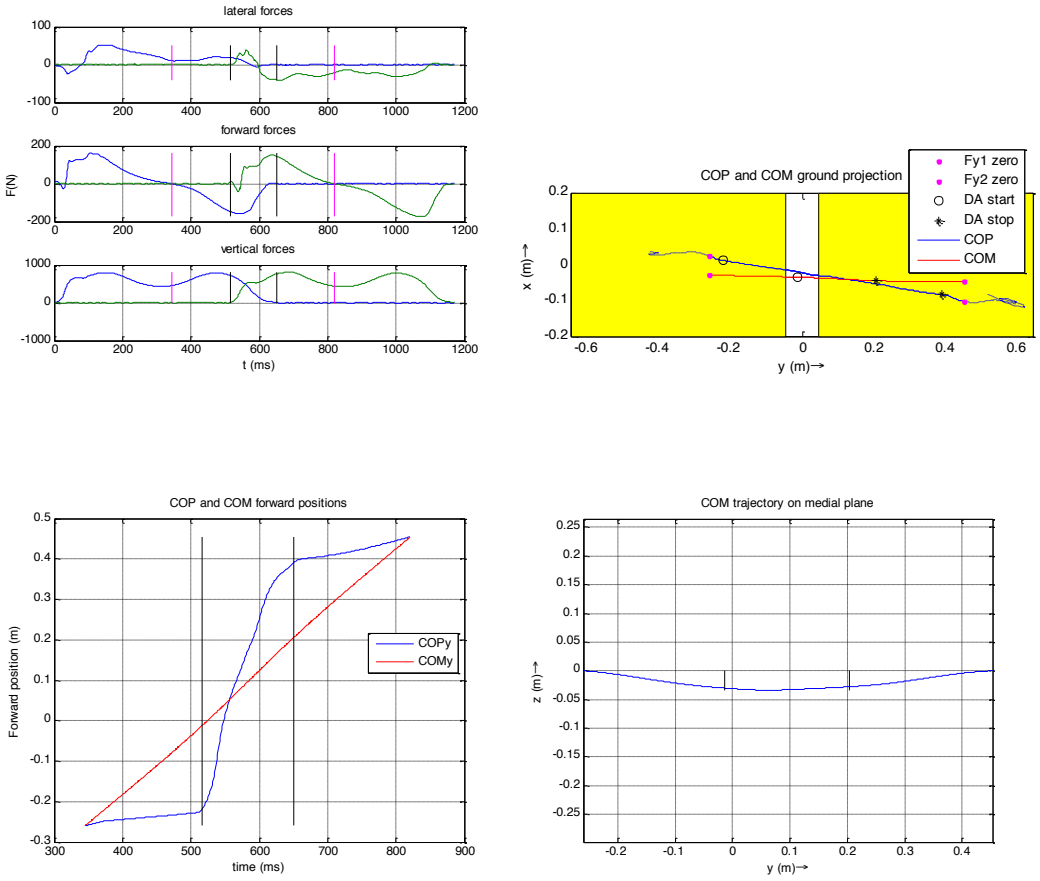

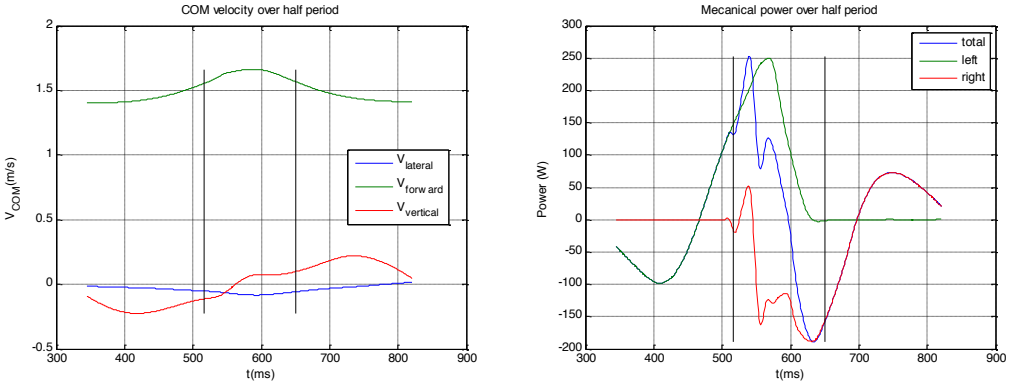

Figure 65 - step analysis of normal gait

The results are as expected with very little lateral and vertical COM displacement and a very symmetrical gait pattern.

These are the results when evaluating pathological gait (Figure 66).

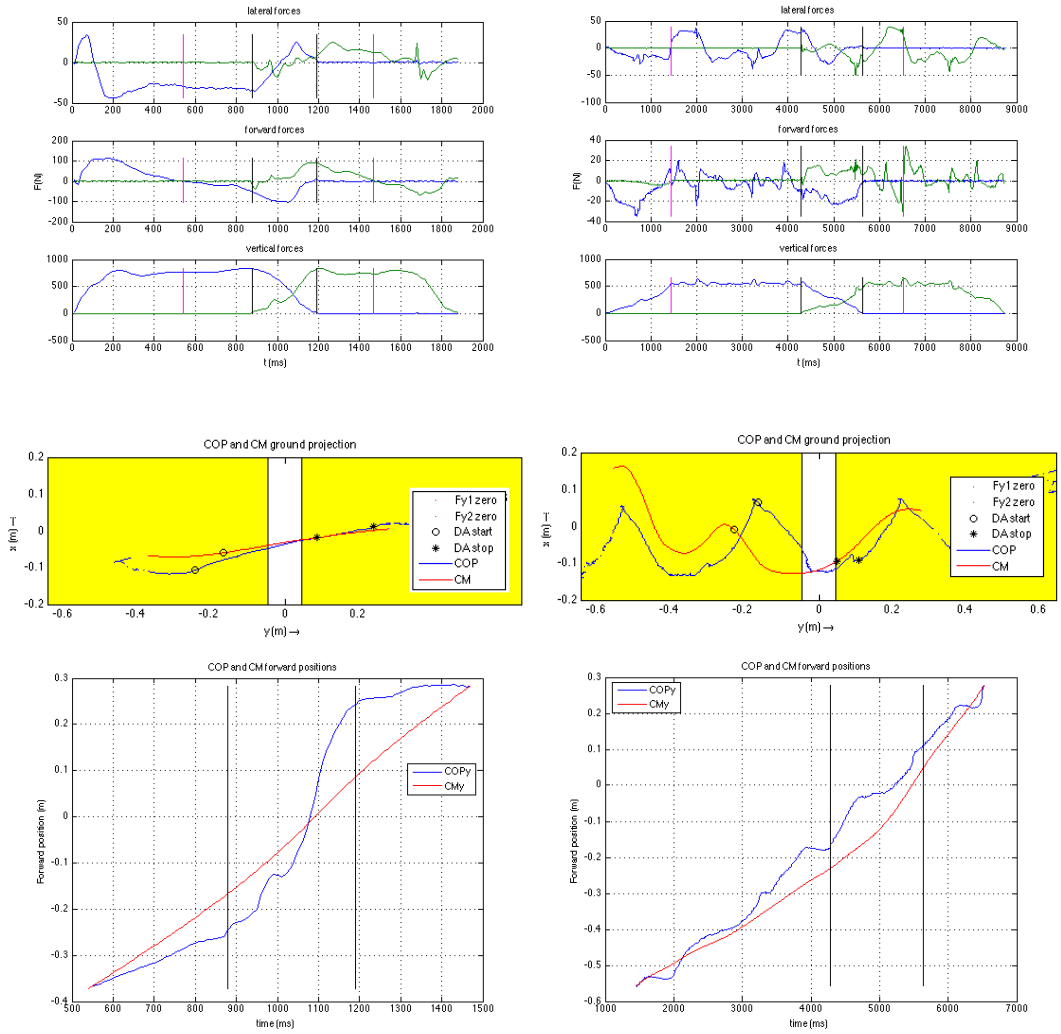

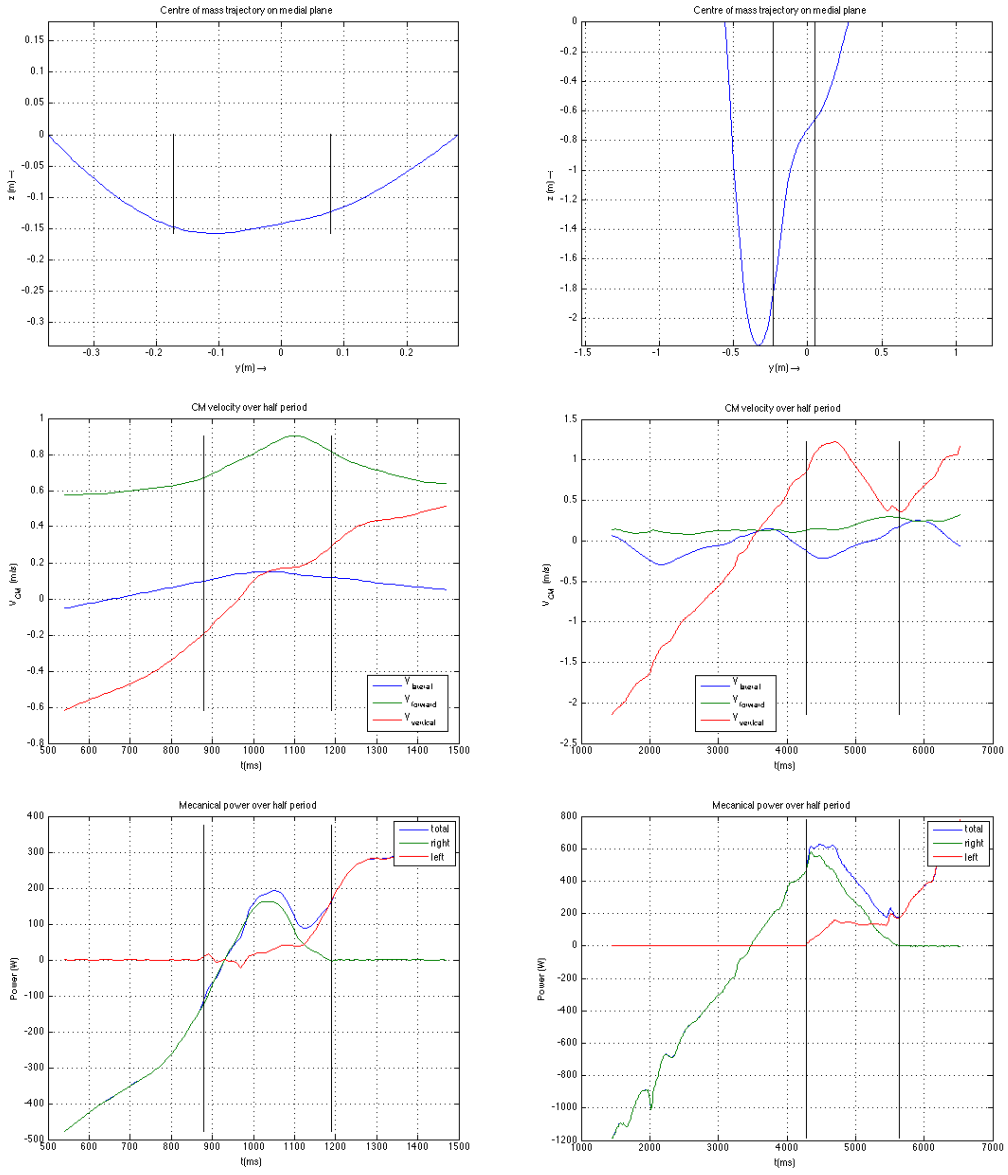

a) b)

Figure 66 - a) step analysis of a pathological gait b) multiple step analysis of a pathological gait

In the example a) a single support per force plate is done and both feet are completely contained in each force plate. From the COPy vs COMy plot is clear the asymmetry. This leads to an increase in the velocity in all three components as seen in the COM velocity plot. Despite that all the parameters are correctly calculated and displayed.

It is clear that example b) is completely inaccurate for all the calculations except for the COP trajectory. This is a result of multiple steps per plate and at least one step that was done partially outside the force plate, so that the GRF could not be correctly measured. The algorithm was not built to deal with multiple steps or partially

measured supports so none of its calculations makes sense. An extension to multiple steps per platform is, however, trivial.

The numerical output for the normal gait case is in Figure 67.

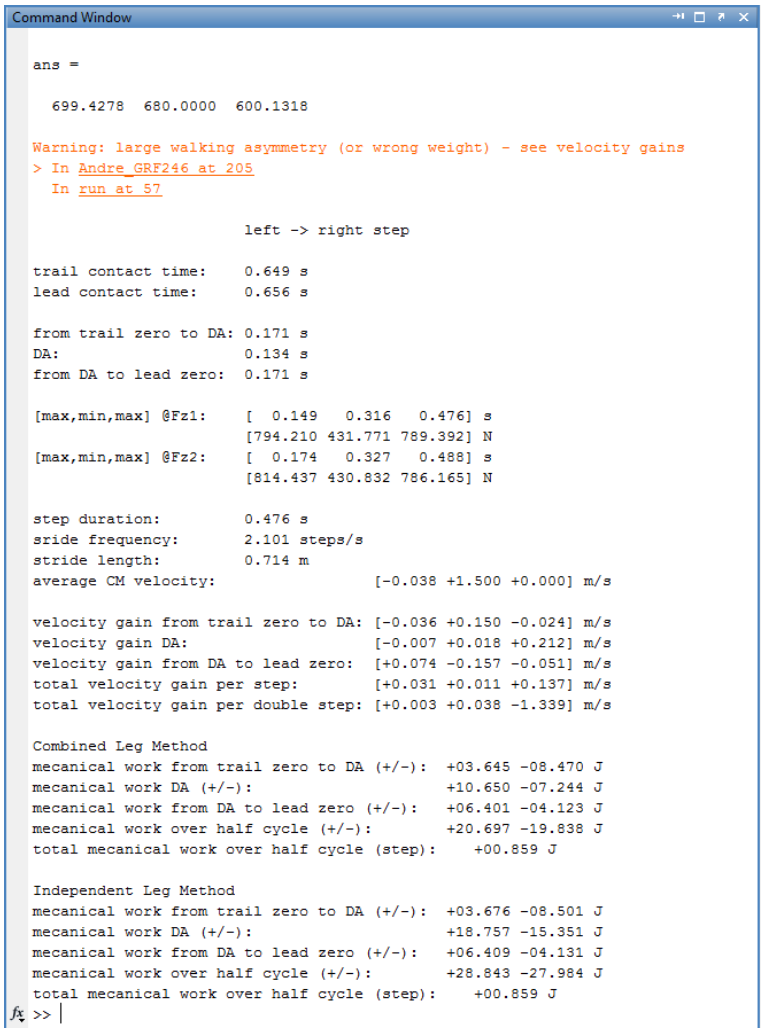

Figure 67 - Output

This output is the numerical representation of some parameters that can help to understand and evaluate gait. It can also be seen the implemented weight/velocity check warning, one of several checks scattered across the program. In this case it probably results from an effort from the subject to *hit* the force plates, changing slightly but measurably its gait pattern.

5.3 – EMG results

The EMG algorithm results consist of a graphic and a numeric output per channel. An example of the graphical output can be seen on Figure 68 and the numerical output on Figure 69.

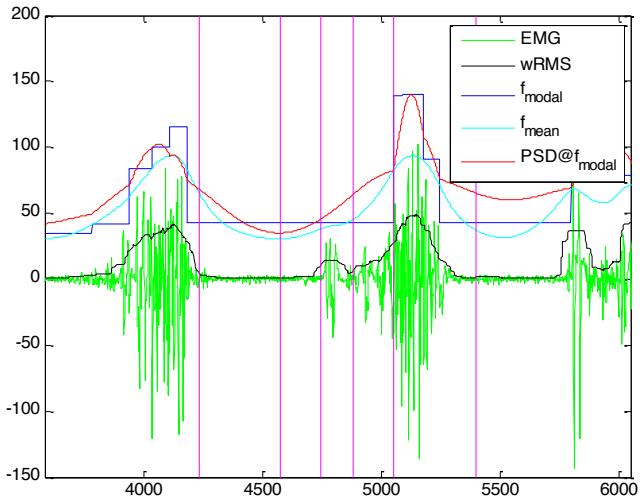

Figure 68 - EMG graphical output

Command Window

```
RMS values for EMG (one line per muscle):
       A      B1      C1       D      DA       E      B2      C2       F
  1 0.0565 0.0436 0.0476 0.0678 0.0925 0.0641 0.0705 0.0518 0.0595
  2 0.0249 0.0179 0.0204 0.0186 0.1781 0.0784 0.2215 0.5751 0.1101
  3 0.1248 0.2571 0.1956 0.2543 0.3534 0.0904 0.2056 0.0680 0.1041
  4 0.0466 0.1428 0.1110 0.0257 0.0592 0.0989 0.1968 0.2717 0.1181
  5 0.0116 0.0136 0.1219 0.0299 0.0231 0.0163 0.0142 0.0148 0.0105
  6 0.0160 0.0149 0.0423 0.1249 0.1694 0.0495 0.0188 0.0256 0.0149
  7 0.0758 0.0112 0.0140 0.0135 0.0388 0.0317 0.0104 0.0162 0.0629
  8 0.0655 0.1946 0.3208 0.0919 0.0239 0.0244 0.0214 0.0224 0.0437
  9 0.2547 0.1796 0.0852 0.0530 0.1015 0.1295 0.1937 0.1904 0.2925
 10 0.1417 0.1249 0.3317 0.2238 0.0443 0.0250 0.0228 0.0227 0.0677
 11 0.0436 0.0207 0.0183 0.0132 0.0111 0.0095 0.0154 0.0866 0.0320
 12 0.2705 0.0222 0.0182 0.0106 0.0155 0.0092 0.0125 0.0416 0.1942
       A      B1      C1       D      DA       E      B2      C2       F
```

Figure 69 - EMG numeric output

The graphic output gives the raw emg signal and the rms envelope. It also calculates the mean and modal frequencies. It displays the main time instants (start, stop and zero).

5.4 – Summary

The obtained results shows that the program can successfully analyze gait data. If the subject is to asymmetrical the COM may have small inaccuracies but all the other

parameters will be correctly displayed. For multiple steps the program can still calculate the COM displacement correctly but all the velocity dependent parameter will be incorrectly displayed

6 – Conclusions and future development

6.1 – Conclusions

The computational tools developed during this work have been successfully implemented. The user interface is simple and easy to use. The code is as autonomous as possible depending only of one external toolbox to implement filters. Also a lot of work was made to reduce (by around 2 orders of magnitude) the computational effort of the wavelet analysis, although full advantage from it is still not possible. The GRF analysis algorithm works for both normal and impaired subjects but the plots concerning COM trajectory may not be displayed correctly if the subject is very asymmetrical. Even so all the other outputs will be correct. The EMG analysis also provides an easy to read output if only a basic analysis is required.

This will, hopefully, aid researchers to improve their gait analysis studies not only by saving time, improving checks on signal quality and by making a comprehensive data analysis.

6.1 – Future developments

Future works could include the adaptation of the code for asymmetrical gait. There two assumptions that are made when calculating the centre of mass displacement and it's velocity that cannot be made if the subject is strongly asymmetrical. For a complete analysis and/or a more accurate evaluation of both healthy and impaired subjects we suggest the use of three force plates. This way we could calculate all the parameters across a stride cycle and evaluate limb asymmetries. Another way of doing this kind of analysis using only two force plates is by placing an incompressible sheet of a hard material (i.e. metal) on top of both platforms. This surface should have the necessary length to take three steps on top of it and the force plates should be located on opposite sides and touching the outermost border of this surface.

Of great interest would be the development of an AI procedure for automatic diagnosis. This would consist of a database containing signal examples of both normal and impaired subjects so it could do an automatic detection of the subject condition (AI based classification).

A more detailed and exhaustive EMG study needs to be made to understand if the wavelet based time-frequency analysis is valuable to calculate activation patterns/times. This would include a large sample and several types of contractions both maximum and sub-maximum, fast and slow, isometric and dynamic, etc. Also this type of analysis could help understand the physiology behind muscular activation.

References

Alem, N. M. and University of Michigan. Transportation Research Institute. (1986). Filter characteristics for processing biomechanical signals from impact tests. Final report. Ann Arbor, Mich., University of Michigan, Transportation Research Institute: 191 p.

Alonso, V. K., S. S. Okaji, et al. (2003) "Análise cinemática da marcha em pacientes hemiparéticos." FisioBrasil, 16-23.

AMTI. (2013). "Force plate components." from http://www.amti.biz/cable-connector.aspx.

Aristotle (n.d.). De Incessu Animalium. The Works of Aristotle translated into English. J. A. Smith and W. D. Ross. London, Oxford at the Clarendon Press. Vol. V.

Auger, F., P. Flandrin, et al. (1995-1996). Time-Frequency Toolbox.

BaileyBio. (2008). "Motor Unit." from http://www.baileybio.com/plogger/?level=picture&id=239.

Basmajian, J. V. and C. J. De Luca (1985). Muscles alive : their functions revealed by electromyography. Baltimore, Williams & Wilkins.

Bawa, P. (2002). "Neural control of motor output: can training change it?" Exerc Sport Sci Rev 30(2): 59-63.

Bio-Medical Instruments, I. (2013). "Surface EMG electrodes." from http://bio-medical.com/media/catalog/product/cache/2/image/600x600/9df78eab33525d08d6e5fb8d27136e95/3/5/35mmarbo.jpg.

Borelli, G. A. (1680-1681). De motu animalium. n.p.,, n.d.

Collins, S., A. Ruina, et al. (2005). "Efficient bipedal robots based on passive-dynamic walkers." Science 307(5712): 1082-1085.

Cook, R. E., I. Schneider, et al. (2003). "Gait analysis alters decision-making in cerebral palsy." J Pediatr Orthop 23(3): 292-295.

De Luca, C. J. (2002) "Surface Electromyography: Detection and Recording ".

DeLuca, P. A., R. B. Davis, 3rd, et al. (1997). "Alterations in surgical decision making in patients with cerebral palsy based on three-dimensional gait analysis." J Pediatr Orthop 17(5): 608-614.

Du Bois-Reymond, E. (1848). Untersuchungen über thierische elektricität. Berlin,, G. Reimer.

Enoka, R. M. (2008). Neuromechanics of human movement. Champaign, IL, Human Kinetics.

Farina, D., R. Merletti, et al. (2004). "The extraction of neural strategies from the surface EMG." J Appl Physiol 96(4): 1486-1495.

Fowler, R. and L. Galvani (1793). Experiments and observations relative to the influence lately discovered by M. Galvani and commonly called animal electricity. Edinburgh, T. Duncan.

Gard, S. A., S. C. Miff, et al. (2004). "Comparison of kinematic and kinetic methods for computing the vertical motion of the body center of mass during walking." Hum Mov Sci 22(6): 597-610.

Ghez, C. and J. W. Krakauer (2000). The organization of movement. Principles of neural science. E. R. Kandel, J. H. Schwartz and T. M. Jessell. New York, McGraw-Hill, Health Professions Division: 653-673.

Horak, F. B. (2006). "Postural orientation and equilibrium: what do we need to know about neural control of balance to prevent falls?" Age Ageing 35 Suppl 2: ii7-ii11.

Júnior, P. F. and J. A. Barela (2006). "Alterações no funcionamento do sistema de controle postural de idosos. Uso da informação visual." Revista Portuguesa de Ciências do Desporto 6(1): 94-105.

Kamisago, M., S. D. Sharma, et al. (2000). "Mutations in sarcomere protein genes as a cause of dilated cardiomyopathy." N Engl J Med 343(23): 1688-1696.

Kernell, D. (2003). "Principles of force gradation in skeletal muscles." Neural Plast 10(1-2): 69-76.

Kirtley, C. (2006). Clinical gait analysis : theory and practice. Edinburgh, Elsevier Churchill Livingstone.

Kuo, A. D. (2007). "The six determinants of gait and the inverted pendulum analogy: A dynamic walking perspective." Hum Mov Sci 26(4): 617-656.

Kuo, A. D. and J. M. Donelan (2010). "Dynamic principles of gait and their clinical implications." Phys Ther 90(2): 157-174.

Ladegaard, J. (2002). "Story of electromyography equipment." Muscle Nerve Suppl 11: S128-133.

Loeb, G. E. and C. Ghez (2000). The motor unit and muscle action. Principles of neural science

E. R. Kandel, J. H. Schwartz and T. M. Jessell. New York, McGraw-Hill, Health Professions Division: 674-693.

Lofterod, B., T. Terjesen, et al. (2007). "Preoperative gait analysis has a substantial effect on orthopedic decision making in children with cerebral palsy: comparison between clinical evaluation and gait analysis in 60 patients." Acta Orthop 78(1): 74-80.

Mackey, D. C. and S. N. Robinovitch (2006). "Mechanisms underlying age-related differences in ability to recover balance with the ankle strategy." Gait Posture 23(1): 59-68.

McGeer, T. (1990). "Passive Dynamic Walking." The International Journal of Robotic Research 9(2): 62-72.

MedicaLook. (2013). "Skeletal muscles." from http://www.medicalook.com/human_anatomy/organs/Skeletal_muscles.html.

Medizintechnik, S. (2013). "EMG needle." from http://www.schulermedshop.com/EMG-electrodes/Concentric-EMG-disposable-needle-electrodes/Concentric-EMG-needle2.

Monteiro, M. D. A. F. (2004). Comportamento postural dinâmico. PhD, U.T.A.D.

Newton, I. (1687). Philosophiæ naturalis principia mathematica. Londini, Jussu Societatis Regiæ ac Typis Josephi Streater. Prostat apud plures Bibliopolas.

Norkin, C. C. and P. K. Levangie (1992). Joint structure & function : a comprehensive analysis. Philadelphia, Davis.

Pais, M. (2005). Efeito de um programa de actividade física no equilíbrio estático e dinâmico em idosos. MSc, UP.

Perry, J. (1992). Gait analysis : normal and pathological function. Thorofare, NJ, SLACK.

Pollo, F. E. (2007). Gait Analysis: Techniques and Recognition of Abnormal Gait. B. U. M. Center.

ProProfs. (2013). "Sarcomere." from http://www.proprofs.com/flashcards/upload/a3922669.gif.

Quach, J. H. (2007). Surface Electromyography: Use, Design & Technological Overview. academic report for Introduction to Biomedical Engineering, University of Concordia, Canada.

Raez, M. B., M. S. Hussain, et al. (2006). "Techniques of EMG signal analysis: detection, processing, classification and applications." Biol Proced Online 8: 11-35.

Rau, G., C. Disselhorst-Klug, et al. (1997). "Noninvasive approach to motor unit characterization: muscle structure, membrane dynamics and neuronal control." J Biomech 30(5): 441-446.

Redi, F. and T. Platt (1686). Esperienze intorno a diverse cose natvrali, e particolarmente a qvelle, che ci son portate dall'Indie. Firenze,, P. Matini.

Rose, J. and J. G. Gamble (1998). Marcha Humana. São Paulo, Editorial Premier.

Saunders, J. B., V. T. Inman, et al. (1953). "The major determinants in normal and pathological gait." J Bone Joint Surg Am 35-A(3): 543-558.

Seeley, R. R., T. D. Stephens, et al. (1995). Anatomy & physiology. St. Louis ; London, Mosby.

Silva, T. C. D. d. (2009). Análise de marcha em mulheres obesas e sua relação com índice de massa corporal. MSc, Universidade de Brasília.

Sousa, A. S. P. d. (2009). Análise da marcha baseada em correlação multifactorial. MSc, Porto University.

Stevens, J. A., P. S. Corso, et al. (2006). "The costs of fatal and non-fatal falls among older adults." Inj Prev 12(5): 290-295.

Stulen, F. B. and C. J. DeLuca (1981). "Frequency parameters of the myoelectric signal as a measure of muscle conduction velocity." IEEE Trans Biomed Eng 28(7): 515-523.

Whittle, M. (2007). Gait analysis : an introduction. Edinburgh ; New York, Butterworth-Heinemann.

Wikipedia. (2005). "Action Potential." from http://en.wikipedia.org/wiki/File:Action_potential_vert.png.

Wikipedia. (2007). "Sarcomere." from http://en.wikipedia.org/wiki/File:Sarcomere.svg.

Winter, D. A. (1990). Biomechanics and motor control of human movement. New York, Wiley.